

Controls on sand ramp formation in southern Namibia

Alex Rowell,^{1*}  David Thomas,¹  Richard Bailey,¹  Abi Stone,²  Eduardo Garzanti³  and Marta Padoan³

¹ School of Geography and the Environment, University of Oxford, Oxford, UK

² Department of Geography, University of Manchester, Manchester, UK

³ Department of Earth and Environmental Sciences, Università di Milano-Bicocca, 20126 Milano, Italy

Received 28 May 2016; Revised 26 March 2017; Accepted 28 March 2017

*Correspondence to: Alex Rowell, University of Oxford, School of Geography and the Environment, South Parks Road, Oxford, OX1 3QY, UK.

E-mail: alexrowell89@gmail.com

This is an open access article under the terms of the Creative Commons Attribution License, which permits use, distribution and reproduction in any medium, provided the original work is properly cited.

ESPL

Earth Surface Processes and Landforms

ABSTRACT: Sand ramps have the potential to provide rich palaeoenvironmental information in dryland regions where proxy records are typically scarce. However, current knowledge of the geomorphic controls and processes of sand ramp formation is limited. This study provides a data-rich examination of the key factors controlling sand ramp formation. The location and morphology of 75 sand ramps in southern Namibia are examined. The sediments and chronologies of 10 sand ramps are studied in detail using 51 OSL dates and 83 grain-size and LOI samples. Heavy mineral assemblages are used to determine the provenance of 10 samples and OSL sensitivity is used to explore geomorphic processes of eight samples.

Sand ramp morphology can be grouped into one of four classes of increasing size and complexity and is closely linked to the available accommodation space. Heavy mineral assemblages indicate local sediment sources and all 75 studied sand ramps are within 4 km of a large ephemeral river channel or within 5.5 km of a dune field. Therefore, accommodation space and sediment supply are identified as the primary controls of sand ramp formation. Sedimentology and OSL sensitivity suggest a complex interplay of aeolian, fluvial and colluvial processes contribute to sand ramp formation with large variability observed between ramps. Three of the ten dated sand ramps have been present in the Namibian landscape for >100 ka. Eight sand ramps show episodic deposition between >75–12 ka and five show evidence of surface reworking over the past 2 ka. Environmental sensitivity is probably linked to the size and availability of the accommodation space. Therefore, individual sand ramps are expected to reflect local environmental conditions, recording when an abundant sediment supply coincided with available accommodation space, while a regional analysis of multiple sand ramps with chronometric data offers the potential to identify larger scale palaeoenvironmental controls of sediment supply. © 2017 The Authors. Earth Surface Processes and Landforms published by John Wiley & Sons Ltd.

Introduction

Studies of Quaternary environmental change in dryland regions are often hampered by a paucity of preserved proxy records (Thomas and Burrough, 2012). The arid climate inhibits the preservation of organic proxies typically used for palaeoenvironmental reconstruction, while ubiquitous 'geoproxy' records (e.g. dunes) can be difficult to interpret in terms of past climatic controls (Chase and Meadows, 2007; Stone and Thomas, 2008; Chase, 2009; Thomas and Burrough, 2012). This is particularly the case in the most arid parts of Namibia, including the Namib Sand Sea, where the analysis of geoproxy archives from within the sand sea has been relatively restricted and sometimes difficult to interpret in palaeoclimatic terms (Lancaster, 2002; Livingstone *et al.*, 2010; Stone, 2013). Geochemical records, from speleothems (Geyh and Heine, 2014), tufa (Stone *et al.*, 2010a), and especially hyrax middens (Chase *et al.*, 2009, 2010; Lim *et al.*, 2016), found in neighbouring Great Escarpment locations have provided alternative data sources that offer more high-resolution datasets.

There are, however, other potential untapped sources of data pertaining to changing environmental conditions in the region. Sand ramps are relatively widespread landforms in drylands which have the potential to provide valuable information on past sediment dynamics (Lancaster and Tchakerian, 1996) but, at present, they are globally under-investigated. Formed when aeolian sediment is trapped against a topographic barrier that also actively contributes to sediment accumulation, sand ramps contain varying proportions of aeolian, hillslope and fluvial sediments (Lancaster and Tchakerian, 1996; Thomas *et al.*, 1997; Bateman *et al.*, 2012). As such, they occupy the continuum between purely aeolian topographic features (e.g. climbing/falling dunes) and purely hillslope deposits (e.g. alluvial fans, talus cones) (Figure 1). As the sediments are derived from different geomorphic processes (that may result from different environmental regimes) and the topographic barrier protects these sediments from remobilisation by subsequent aeolian transport, sand ramps have the potential to provide long and detailed palaeoenvironmental records which can be independently dated using OSL. However, not much is known in detail about the geomorphic controls and

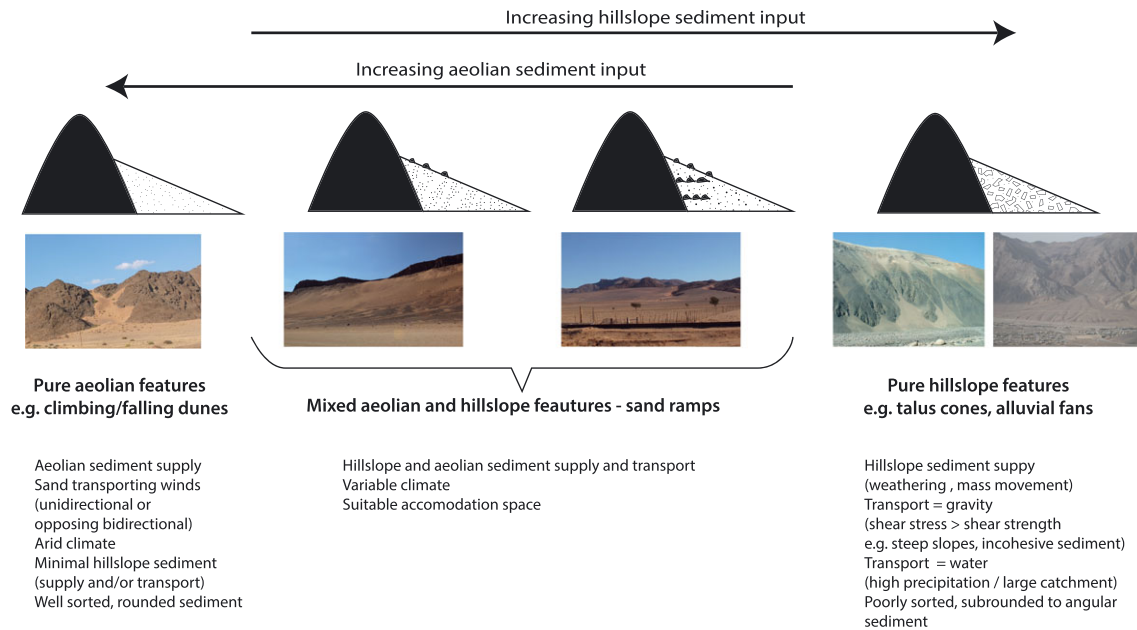


Figure 1. Summary of the main conditions needed for sand ramp formation and the relationship between sand ramps, and aeolian and hillslope features. [Colour figure can be viewed at wileyonlinelibrary.com]

processes that govern sand ramp formation and their interdigitated sedimentary units, and whether variations in climatic forcing are clearly recorded. As such their current utility as palaeoenvironmental archives is limited.

Previous sand ramp studies

At present, only limited research into sand ramps has been undertaken. The majority of this work has been conducted in the Mojave Desert, USA (Lancaster and Tchakerian, 1996; Rendell and Sheffer, 1996; Pease and Tchakerian, 2003; Bateman *et al.*, 2012) but studies also exist from African, Middle Eastern, Asian and European and other American drylands (Clemmensen *et al.*, 1997; Thomas *et al.*, 1997; Turner and Makhoulouf, 2002; Bertram, 2003; Berking and Schütt, 2011; Telfer *et al.*, 2012, 2014; Ellwein *et al.*, 2015; Kumar *et al.*, 2016; del Valle *et al.*, 2016). Table I summarises work to date.

The sand ramps in these investigations embrace a range of geomorphological contexts and sedimentological differences (Table I). Sand ramps require a suitable accommodation space (i.e. a hillslope against which aeolian and colluvial sediments can accumulate) and contain a combination of aeolian and colluvial deposits, but in varying proportions. Both climbing (up wind of a topographic barrier) and falling (downwind) sand ramps have been described. Falling ramps are typically smaller, positioned higher on mountain slopes with steeper slope angles, and with better sorted, finer sediments (Lancaster and Tchakerian, 1996). Gullies have been observed in many sand ramp contexts. These run parallel to the axis of the sand ramp body or are found separating the ramp from the hillslope against which it has accumulated (Lancaster and Tchakerian, 1996; Thomas *et al.*, 1997; Bertram, 2003; Bateman *et al.*, 2012). Both gully types are assumed to post-date accumulation of the main sand ramp body and are generally interpreted to be formed by fluvial activity (Lancaster and Tchakerian, 1996; Bertram, 2003), although aeolian scour has also been suggested as the origin of the latter type (Lancaster and Tchakerian, 1996). The origin of sediments within a sand ramp has important implications for the antecedent conditions needed for formation. Colluvial, talus and fluvial sediments must be derived locally from the adjacent topographic obstacle

(Lancaster and Tchakerian, 1996; Turner and Makhoulouf, 2002; Pease and Tchakerian, 2003). Aeolian units are also suggested to be locally sourced from neighbouring ephemeral channels or proximal upwind playas or dunefields (Bertram, 2003; Pease and Tchakerian, 2003; Bateman *et al.*, 2012), but may also incorporate further-travelled sediment (Thomas *et al.*, 1997).

Chronometric data are available for some sand ramps, giving indications of the timing and age of accumulation (Table I). However, some studies provide complex or conflicting data from the same location. TL and IRSL ages from sand units bracketing stone layers in Mojave ramps showed some to represent up to 10 ka breaks in aeolian unit accumulation, while others indicated no significant temporal breaks in accumulation (Rendell and Sheffer, 1996). The Soldier Mountain sand ramp (Mojave) was originally dated to c.10–22 ka using quartz and feldspar TL and feldspar IRSL dating (Rendell and Sheffer, 1996) and the sediments were interpreted as containing six palaeosols (Lancaster and Tchakerian, 1996). A more recent investigation of this feature, utilising SAR OSL dating, suggested rapid accumulation between c.11.6 and 10.3 ka. No evidence of palaeosol development was found and stone layers were not associated with temporal hiatuses. Rates of modern stone movement on the surface could not be reconciled with the rapid emplacement of stone layers indicated from OSL dating. Deposition of this sand ramp was therefore reinterpreted as opportunistic and event-driven with stone layers suggested to be deposited by periodic small streams distributing the stones across the sand ramp (Bateman *et al.*, 2012).

Rapid deposition was also suggested at the Ardakan sand ramp, Iran (~25 m of sediment deposited between 25 and 20 ka) (Thomas *et al.*, 1997), and for modern sand ramps in Jordan (Turner and Makhoulouf, 2002). However, sand ramps from the Black Mesa, USA, Golden Gate, South Africa and the Ladakh Desert, India potentially suggest episodic deposition between c. 28–9 ka, c.45–7 ka and c.44–8 ka, respectively (Telfer *et al.*, 2012; Ellwein *et al.*, 2015; Kumar *et al.*, 2016). In Eivissa, Western Mediterranean accumulation is correlated with glacial sea level change and associated sediment availability (del Valle *et al.*, 2016). Dates from Namibian sand ramps indicate activity at >100 ka and c.15 ka (Bertram, 2003).

This review suggests that sand ramps are complex and varied features, differing in formation history, and in the relative

Table 1. Summary of previous sand ramp research

Study & location	#	L (m)	T (m)	C/F	Sedimentology	Talus mantle	Gullies	Origin of sands	Chronology	Interpretation	Other
Lancaster and Tchakerian, 1996, Rendell and Sheffer, 1996, Pease and Tchakerian, 2003 Mojave Desert, USA	13	100–2000	5–70	C&F	All predominately aeolian with varying proportions of fluvial, talus and debris flow sediments. No clear regional pattern. Some palaeosols and calcrete formation.	On most ramps. More developed adjacent to steep metamorphic slopes.	Some ramps separated from hillslope.	Geochemistry indicates local fluvial/playa source which has altered though time.	49 MAAR quartz and feldspar TL and SAAD feldspar IRSL dates of varying accuracy. Suggest predominantly episodic deposition between 0 and 45 ka.	Different units represent discrete climatic periods. Talus accumulations within the ramp represent periods of stability. Dates suggest correlation to periods of increased fluvial activity, suggesting sediment supply is the key control on formation. Lack of Late Holocene dates are assumed a result of increased aridity.	Most relic, some currently active.
Bateman <i>et al.</i>, 2012 Soldier Mountain - Mojave Desert, USA	1	n/m	~25	C	Mix of cross-bedded aeolian sands, discontinuous clast layers and calcrete layers.	Tightly packed angular clasts clast-size decreases downslope.	Several gullies dissect the sand ramp laterally.	Nearby (0.5 km) Mojave River assumed to be main source.	6 quartz SAR OSL dates. Sand ramp dates are between 11.6 +/- 0.8–9.5 +/- 0.6 ka. Stone horizons formed in a maximum of 1.8 ka.	Sand ramps form quickly in a “window of opportunity” when accommodation space and sediment supply are both available. They do not represent a simple model of discrete climatic events. Stone layers do not necessarily represent former land surfaces and periods of climatic stability. Instead, they are likely formed by high-magnitude, low-frequency events with some redistribution via fluvial-aeolian creep.	Free dunes on top of ramp.
Ellwein <i>et al.</i>, 2015 Black Mesa, Arizona, USA	3	n/m	>12	C&F	75% Aeolian sands – well sorted with cross-bedding. Interspersed with alluvium and colluvium	no	no	Assumed to be local river channels	7 quartz SAR OSL dates. Top 6 m of sand deposited between 16.2 +/- 1.14–1.9 +/- 0.2 (majority before 7.9 +/- 0.55).	Associated with climatic variability under cooler, wetter, windier conditions than present.	Suggest sand ramps should be defined by morphology i.e. gently sloping wedges against a topographic barrier
Clemmensen <i>et al.</i>, 1997 Mallorca, Western Mediterranean	1	40	20	C	Predominantly aeolian dune sands interspersed with scree deposits.	no	no	Beach sands	n/a	n/a	n/a

(Continues)

Table 1. (Continued)

Study & location	#	L (m)	T (m)	C/F	Sedimentology	Talus mantle	Gullies	Origin of sands	Chronology	Interpretation	Other
Thomas <i>et al.</i>, 1997 Ardakan, Iran	1		25	C&F	Predominantly cross-bedded aeolian with clastic layers up to 40 cm thick.	30 cm of mixed rock fragments and sand.	Dissects sand ramp from hillslope	No modern sediment supply. Assumed ephemeral river channels to the SE under changed wind regimes.	7 MAAD and SAAD quartz samples. All 25–18 ka	Rapid accumulation in a single episode associated with the LGM. Units do not represent different climatic regimes. Wind dynamics during formation were likely different to present. Associated with cold dry conditions	Suggest sand ramps have low angle surfaces compared to obstacle dunes
Turner and Makhoul, 2002 Badia, Jordan	5	10–20	n/m	C	Primarily colluvium from adjacent sandstone. Small aeolian contribution.	n/m	n/m	Adjacent cliffs	Observation – rapid current accumulation	Sand ramps form rapidly from rockfall, grain flow and debris flow events. Increased proportions of rockfall sediments may indicate moisture availability as grainflows are inhibited by moisture. Formation controlled by sediment supply. Deposition associated with aridity during the Last Glacial	Contemporary accumulation
Berking and Schütt 2011 Northern Sudan	4	200–500	n/m	C&F	Predominantly aeolian with talus mantle	Thin layer of pebbles and gravels	Dissect sand ramps from hillslope and downslope	n/m	10 Quartz SAR OSL dates taken from the top 1.3 m of 4 sites. Ages between 0.06 ± 0.02 – 38 ± 5 ka.	Formation is a process of sediment mixing: sand blown upslope by aeolian processes and washed down by heavy rain which also deposits bedrock clasts. Sand ramps form under strong winds and flashy rainfall before stabilising under low intensity rainfall and weak winds. Accumulation occurred in a single phase for small ramps but over at least 8 phases for large Aus ramp.	Dunes overlaying some sand ramps
Bertram, 2003 Namib Desert, Namibia	5*	280–2000	Up to 140	C	Primarily aeolian sands with discrete clastic layers and sporadic clasts. Evidence of palaeosols, calcrete nodules on smaller ramps and multiple calcrete layers on large Aus ramp	On the majority of ramps	Dissect sand ramps from hillslope. Aus is also dissected downslope	Assumed ephemeral river channels and weathering of adjacent bedrock	3 SAR IRSL dates Aus dated to 106.1 ± 7.9 at 3 m and 104.9 ± 8.7 at 7 m. Overlying dunes dated to 15.0 ± 1.1		

(Continues)

Table 1. (Continued)

Study & location	#	L (m)	T (m)	C/F	Sedimentology	Talus mantle	Gullies	Origin of sands	Chronology	Interpretation	Other
Telfer <i>et al.</i>, 2012 Golden Gate National Park, South Africa	1		11	C	Predominantly well sorted fine sands with some cross-bedding interdigitating with discrete clast units and lenses	no	Extensive downslope gullying, badland topography.	Assumed periglacial weathering of local geology	6 quartz SAR OSL dates. 45 ± 3.0 ka – 7.6 ± 0.6 ka.	Deposition is likely to be episodic. Rapid accumulation associated with increased aeolian activity during the LGM linked to increased sediment supply from periglacial weathering and increased windiness. Holocene date is thought to represent colluvial reworking.	
Kumar <i>et al.</i>, 2016 , Ladakh Desert, India	5	Total area: $40\text{--}2000\text{ m}^2$	4–25	C	Varying layers of aeolian sand, fluvial gravels, playa clays and hard crusts containing rock debris.	Found at 3 ramps	Present but no details	Indus fluvial sediments in the pre-monsoon season.	14 Quartz SAR OSL dates. Suggest periods of deposition 25–15 ka and 12–8 ka. Single date at $\sim 44 \pm 3$ ka	Record of wet/dry climate. Aeolian deposits represent arid periods and fluvial sediments intra-dune playas and hiatuses represent wet conditions. Shows good agreement with regional climate reconstructions of wet periods.	Overlying dunes at one ramp.
del Valle <i>et al.</i>, 2016 Eivissa, Western Mediterranean	1	1000 width		C	Calcareous aeolian deposits interbedded with colluvial deposits and palaeosols	n/m	n/m	Beach sand exposed during glacial low sea-level stands	4 OSL dates. 143 ± 8 ka (MIS 6), 100 ± 6 ka (MIS5d/c), 77 ± 5 ka and 73 ± 5 ka. (MIS 4).	Aeolian activity controlled by sediment supply. Associated with low sealevel during glacial periods. Colluvium and palaeosols develop during interglacials.	

- Number of studied sand ramps

L - Length

T - Thickness

C or F - climbing or falling.

n/m - not mentioned in text

*Unspecified number of sand ramps were observed and described. Five sites (including complexes) were studied in detail.

contributions from different sedimentary processes to the final landform. However, most investigations to date have been conducted on single features (Thomas *et al.*, 1997; Bateman *et al.*, 2012; Telfer *et al.*, 2012), such that it is unclear how representative of wider conditions their conclusions are. While the overall processes of ramp accumulation (aeolian, fluvial and slope processes) are largely agreed upon, there are components of ramp systems that are currently poorly investigated or explained. Understanding the timescale and mechanism of sand ramp formation has important implications for palaeoenvironmental reconstructions with opportunistic, single-event driven accumulation providing limited regional information. Meanwhile, the provenance of the aeolian sediment is important for interpreting transport histories (Pease and Tchakerian, 2003) and understanding the environmental significance of the deposit.

This study aims to better understand the controls and mechanisms of sand ramp formation and to evaluate their potential as a palaeoenvironmental archive. This is achieved by conducting: (i) a systematic regional survey of the locations and broad morphologies of sand ramps in south-west Namibia; and (ii) a detailed examination of the morphology, sedimentology, sediment provenance and chronology of a morphologically varied subset of these sand ramps. The combination of heavy mineral analysis and luminescence characteristics (sensitivity) offers an important novel insight into provenance of the aeolian component of sand ramp sediments.

Study Site

The study was conducted in south-west Namibia between 23° and 28°S, and 15° and 18.5°E (Figure 2). This area encompasses the transitional zone between the Great Escarpment, where sand supply is limited, and the hyper-arid sandy coastal plain where sediment supply is high but topographic obstacles are rare. In the intermediate zone of the western foreland of the Great Escarpment both sand supply and topographic obstacles, especially inselbergs, are sufficient to lead to the presence of numerous sand ramps in a variety of accommodation spaces

(Bertram, 2003). Exposed lithologies are of mixed erodibility with sandstones, limestones and shales prevalent in the region (Atlas of Namibia Project, 2002; Figure 2 inset).

Western Namibia has an arid to hyperarid climate, primarily due to a dominant subtropical atmospheric high pressure regime and the limited incursion of moisture from easterly sources. This is enhanced in the coastal zone by upwelling of the cold Benguela current, which further cools the atmosphere inhibiting precipitation other than fog development. Consequently a steep W–E precipitation gradient (barely above 0 to 200 mm), high inter- and intra-annual variability are key features of the regional climate (Lancaster *et al.*, 1984; Nicholson, 2000). Wind regimes are bimodal. Prevailing winds from the S–SW dominate for most of the year reaching maximum strength (up to 14 ms^{-1} at the coast, reducing inland) in early Austral summer (September–November) (Lancaster, 1985). E to NE katabatic, mountain-to-plain winds are frequent in Austral winter (June–August) (Tyson and Seely, 1980). When regional pressure gradients are normal to the coast these can develop into strong easterly ‘berg’ winds. These frequently reach velocities of $14\text{--}17 \text{ ms}^{-1}$ and can account for up to 65% of total sand transport on the northern and eastern margins of the Namib Sand Sea, although their strength rapidly decreases towards the west (Lancaster *et al.*, 1984; Lancaster, 1985). The range of geological and morphological settings, E–W precipitation gradient, and wind dynamics in the study area provide prime test conditions for assessing the controls on sand ramp formation.

Methods

Sand ramp identification and selection

Sand ramps were primarily identified using Google Earth™ satellite imagery, much with a 15–30 m (derived from Landsat imagery) or finer (CNES/Astrium and Digitalglobe) resolution.

The identification of sand ramps was an iterative process. The aerial morphology of previously studied ramps (Lancaster and Tchakerian, 1996; Bertram, 2003; Bateman *et al.*, 2012) was

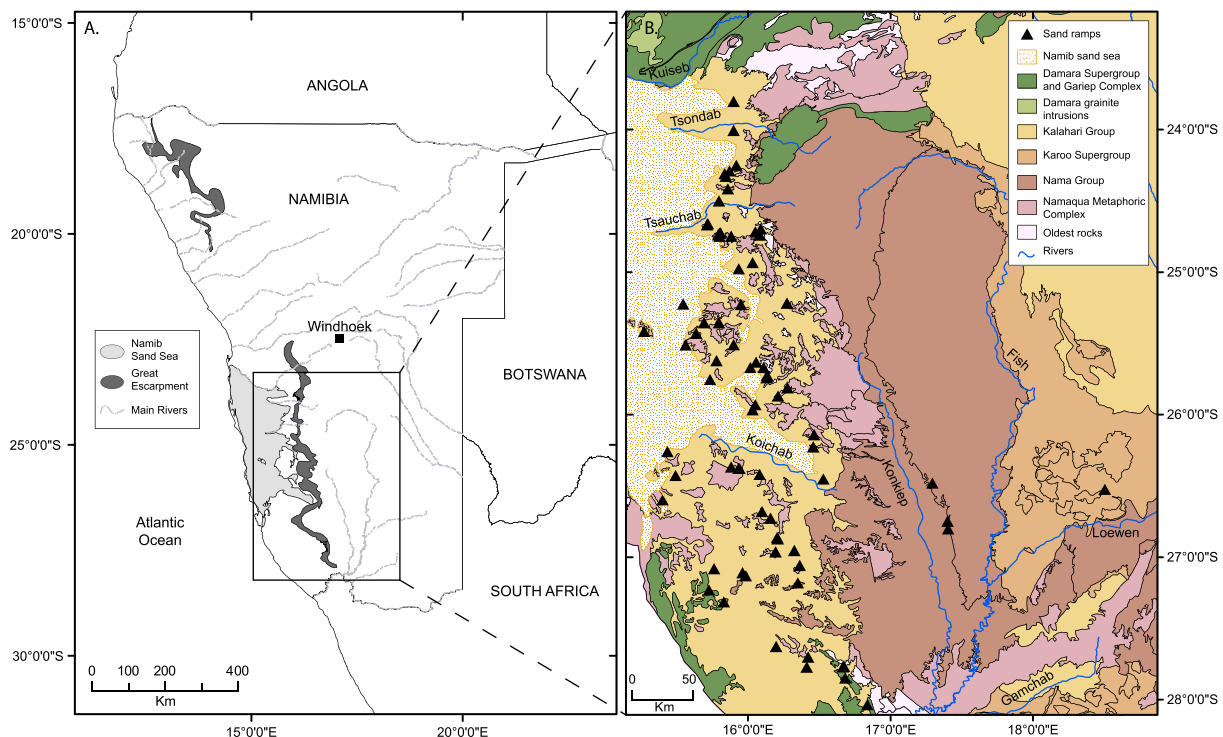


Figure 2. Location of study area (A) and sand ramps in geological context (B). [Colour figure can be viewed at wileyonlinelibrary.com]

initially used as a reference training set and all potential ramps in the study area were identified. Features were identified by first locating potential accommodation spaces (hillslopes and topographic barriers) using systematic scanning and secondly by searching for accumulations of sand against these mountains. The simple regional geomorphology of inselbergs within a plain and low vegetation cover meant potential accommodation spaces and sand accumulations were relatively easy to identify. Ground-truthing was conducted on a subset of the potential sand ramps. This highlighted that some features identified aerially were only thin sand drapes at ground level while some features were easy to identify on the ground but overlooked in aerial surveys (Figure 3). Following this, 57 sand ramps were removed from the inventory based on ground level information or unclear aerial morphology while six previously unidentified features were added. When present, gullies gave a good indication of sand ramp thickness. Of the 75 remaining sand ramps in the inventory approximately 70% were verified in the field. The remaining 30% were inaccessible at ground level but had clear sand ramp aerial morphology.

Aerial imagery and field observations revealed that while sand ramp morphology exists along a continuum, there are four recognizable broad groupings of these features (Table II). A (nested) classification system was developed to test whether morphological characteristics could be used as a predictor of the accumulation history (and maximum age) of the sand ramps.

Sand ramps were initially classified based on the presence/absence of morphological features such that: class 1 are connected to the hillslope with a unconsolidated sand surface and no secondary dune features on the surface; class 2 are disconnected from the hillslope by a gully, often with a vegetated surface but no secondary dune features; class 3 are disconnected from the hillslope by a gully, often with an indurated surface that is well-vegetated and overlying secondary dune features; and class 4 are disconnected from the hillslopes by a large gully, frequently with a duricrust surface and presence of overlying secondary dunes. Following this classification, a relationship between size and morphology emerged with size increasing with morphological class (Table II). We therefore hypothesise that size (related to available accommodation space) and increasing morphological complexity will be positively correlated with the length of the accumulation history preserved.

Ten sand ramps were selected for detailed investigation in the field. Sites were chosen to reflect a variety of the identified characteristics (three are class 1, two class 2, two class 3 and three class 4) (Figure 4). The majority of these features had natural exposures, formed by gullying, which allowed sedimentary structures to be observed in detail. In these cases, OSL samples were taken by hammering opaque tubes into cleaned faces. Samples were taken to provide depositional ages for sedimentary units: (i) to bracket changes in sedimentary features (e.g. stone layers); and (ii) where the sediment was relatively homogenous, a resolution of ~1 m was used to assess accumulation history. For large exposures (e.g. Sarama) sampling was restricted by accessibility and resolution reduced accordingly. When gullies were not available (e.g. Neuhoof-1) hand-dug pits were used to examine the sedimentology of the top ~2 m of sand ramps sediments and samples were taken to bracket changes in sedimentary features or at a resolution of ~0.5 m (sampling resolution was reduced due to the smaller size of exposures). The dunes overlaying class 3 and class 4 sand ramps were sampled to assess their relationship with the sediments of the main sand ramp. Samples were taken from hand augured holes up to 5 m deep using a Dormer™ portable auger adapted for OSL sampling (Telfer and Thomas, 2007). Samples were taken at

~1 m resolution although depth of sampling was frequently limited to the top ~2 m due to poor sand cohesion.

Sedimentological analysis

Field-logging of exposures was undertaken, including broad descriptions of sediment composition in different units. Material from the ends of OSL sample tubes were used for sedimentological analysis. Particle size analysis of the <2 mm size fraction was conducted using a Malvern Laser Granulometer Hydro Mu 2000 using wet dispersion and ultrasonic diffusion (pilot tests indicated pretreatment to remove organics and carbonates was unnecessary). Statistics were calculated using the Folk and Ward (1957) formula and the GRADISTAT™ program (Blott and Pye, 2001). The >2 mm fraction was not measured. Percentage carbonate and organic content were calculated using sequential loss on ignition at 550°C and 950°C (Heiri *et al.*, 2001).

Analysis of heavy mineral assemblages provides constraints on the mineralogy of the sediment source and therefore can be used to identify the most likely sediment provenance (Morton and Hallsworth, 1999). Heavy mineral analysis was conducted at the University of Milano-Bicocca. Heavy minerals were separated using sodium polytungstate (density ~2.90 g/cm³). After mounting with Canada balsam, ≥200 transparent heavy-mineral grains were point-counted to obtain real volume percentages (Galehouse, 1971). Heavy-mineral concentration was calculated as the weight percentage of total (HMC) and transparent (tHMC) heavy minerals relative to the bulk-sediment sample (Garzanti and Andò, 2007). Variance between sand ramps samples, and samples from the Namib Sand Sea and major Namibian ephemeral rivers (see Garzanti *et al.*, 2012 for sample details) was assessed using un-scaled principle component analysis (PCA) (see Wold *et al.*, 1987).

OSL sample preparation and measurement

All samples were prepared under subdued orange light at the Oxford Luminescence Dating Laboratory. The quartz fraction was isolated to 90–125 µm for dating and 180–210 µm for sensitivity experiments, using treatment with H₂O₂ and HCl, density separation using sodium polytungstate to 2.58–2.72 g/cm³ wet sieving and a 60 min etch in 40% HF. 14 samples were also treated with H₂SiF₆ for 7–14 days to remove persistent feldspar contamination.

All luminescence measurements were conducted using a Risø TL/OSL-DA-15 automated reader (Bøtter-Jensen *et al.*, 2003) fitted with either blue (470 nm) or green (525 nm) LED array. Infra-red (IR) simulation was conducted using a 870 nm laser diode array. Luminescence was measured using an EMI9235QA photomultiplier fitted with 7 mm of Hoya U-340 filters. Beta irradiation was administered using 90Sr/90Y beta sources calibrated relative to the National Physical Laboratory, Teddington Hotspot 800 60Co γ-source (Armitage and Bailey, 2005).

Typically, 24 small aliquots (~500 grains, Duller, 2008) were measured using a modified single aliquot regeneration (SAR) protocol (Wintle and Murray, 2006). Preheats (PH1–260°C for 10 s and PH2–220°C for 10 s) were determined following preheat plateau tests on recovered doses from a subset of samples (Supplementary information 1). OSL was measured at 130°C for 40 s or 100 s (blue or green diodes, respectively). Each SAR cycle was followed by a 280°C optical bleach for 40 s or 100 s. A repeated dose (recycling ratio; RR point) was

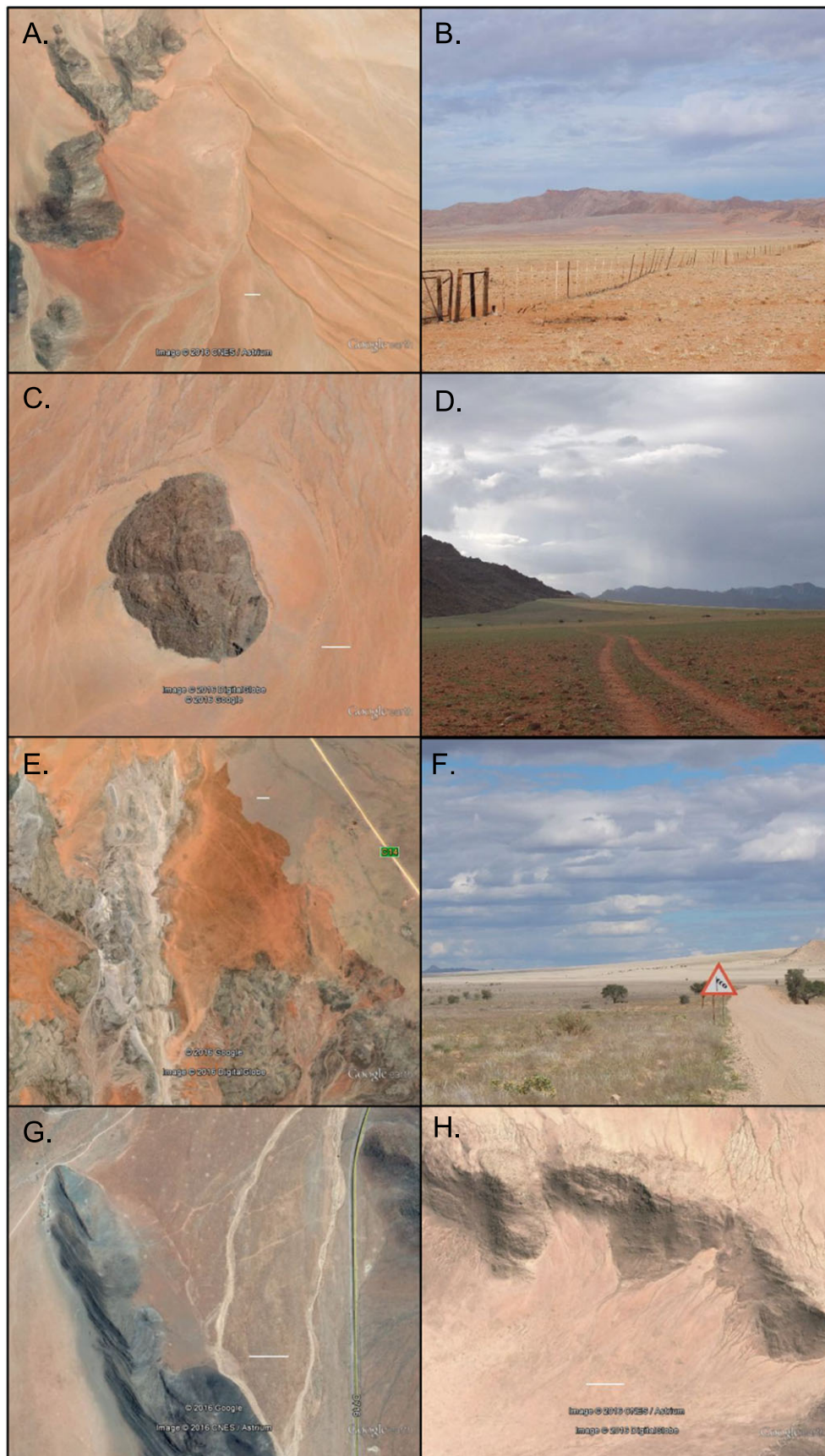


Figure 3. Examples of sand ramps identified using Google Earth™ and confirmed in the field (A–D; A and C are Google Earth™ images, B and D are the respective features from the ground). Example of a sand ramp identified in the field but not initially found using Google Earth™ (E & F; E is the Google Earth™ image, F is the field view). Examples of features identified using Google Earth™ but found to be thin sand drapes (G & H). [Colour figure can be viewed at wileyonlinelibrary.com]

Table II. Sand ramp morphological classification

Class	Morphological characteristics			Schematic and example
	Size	Connected to hillslope	Surface characteristics	
1	Small Length: 150–500 m Width: 300–900 m	Connected	Sands are unconsolidated but will hold a face Evidence of recent aeolian activity.	No secondary features
2	Medium Length: 300–800 m Width: 300–800 m	Disconnected by a channel or gully	Sands are unconsolidated but will hold a face Often well vegetated	No secondary features
3	Medium to large Length: 1000–1500 m Width: 1000–1750 m	Disconnected by channel or gully	Well vegetated Often indurated	Loose sand ridges/dunes overlay the sand ramp
4	Large Length: 1500–3000 m Width: 1500–3550 m	Disconnected by a large gully.	Contain duricrusts Consolidated sand ramp sediments	Overlying dunes present

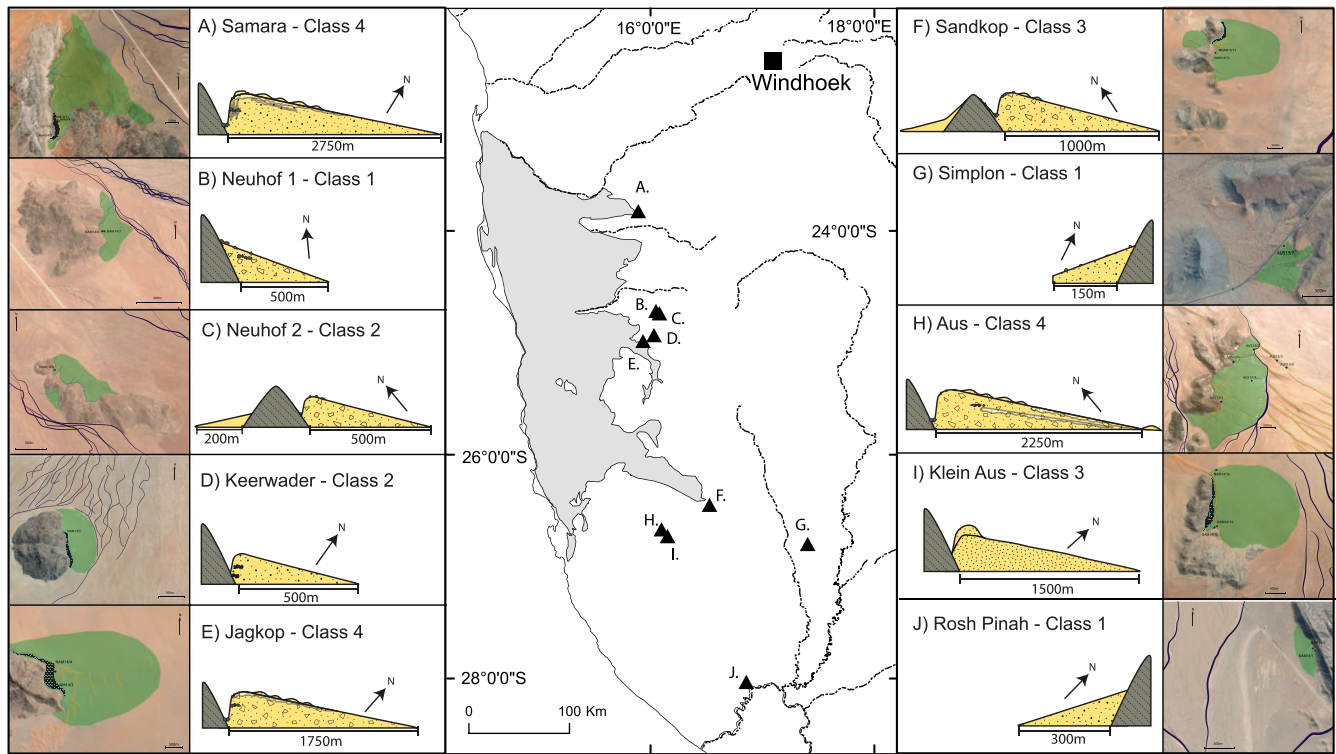


Figure 4. Location and morphology of dated sand ramps. Plan views are shown on the far right and far left; green shaded areas represent the extent of the sand ramps, blue lines highlight river channels. Schematic representations of the sediments and morphology of the ramps are depicted in the inner left and inner right panels. [Colour figure can be viewed at wileyonlinelibrary.com]

included to monitor sensitivity change and an IR-depletion ratio point (Duller, 2003) was included to test for feldspar contamination. Recuperation was monitored using a zero point. Samples were rejected if repeat RR or IR points were $>10\%$ of unity, recuperation was $>5\%$ of the natural signal or samples had a fast ratio <20 (Durcan and Duller, 2011). Dose recovery tests (DRTs) were performed on a subset of samples. Before irradiation to magnitudes similar to the equivalent dose, discs were twice bleached for 1000 s at 20°C separated by a 10 000 s pause. All measured samples recovered the given dose within 10% (Supplementary information 1).

Dose response curves (DRCs) were fitted with the most appropriate of a single saturating exponential (SSE), saturating exponential plus linear (SEPL) or double saturating exponential (DSE) function. Individual D_e estimates were derived using interpolation of the natural onto this curve. Uncertainties were calculated using 1000 Monte Carlo fits of the curve and propagated with a 2% measurement error. Sample D_e s were calculated using the Central Age Model (CAM) (Galbraith, 1999).

Radionuclide (^{232}Th , ^{238}U and ^{40}K) concentrations of all samples were measured using ICP-MS (^{232}Th and ^{238}U) and ICP-OES (^{40}K). Where available, gamma spectrometry was used to determine the gamma contribution. Radionuclide concentrations were calculated using the window method (Aitken, 1985). Radioactivity was calculated using the Liritzis *et al.* (2013) conversion factors. Based on the aridity of the modern climate, values used in previous studies in the region (Bristow *et al.*, 2005, 2007; Stone and Thomas, 2008; Stone *et al.*, 2010b) and the position of samples (either free draining slopes with evidence of fluvial activity or dunes) a water value of $5 \pm 3\%$ was used for all samples. Beta attenuation was corrected for using Guérin *et al.* (2012) and the etch depth values of Bell (1979). Cosmic dose was calculated using the formula of Prescott and Hutton (1994). Total dose rates were calculated using DRAC (Durcan *et al.*, 2015).

Luminescence sensitivity tests

The sensitivity of quartz (counts produced per given dose) can provide insights into the environmental history of a sediment sample. This is based on three observations: (i) quartz is sensitised in nature and the laboratory through repeated cycles of signal accumulation and bleaching without heating (Moska and Murray, 2006; Pietsch *et al.*, 2008; Fitzsimmons *et al.*, 2010); (ii) sensitivity increases significantly after heating to 500°C in the laboratory (Bøtter-Jensen *et al.*, 1995; Poolton *et al.*, 2000); and (iii) sensitivity changes due to heating to 500°C are dependent on initial sample sensitivity, with already-sensitised quartz undergoing a subdued sensitivity increase (Moska and Murray, 2006). Therefore, grains that have undergone repeated burial and bleaching cycles in nature, including through aeolian processes, produce more luminescence for a given dose than freshly weathered quartz (Pietsch *et al.*, 2008; Fitzsimmons *et al.*, 2010; Sawakuchi *et al.*, 2011a) and are less likely to undergo very large sensitivity changes after heating (Moska and Murray, 2006). This approach is particularly relevant for sand ramps that result from multiple depositional processes including colluvium that may be relatively freshly weathered from the topographic barrier and aeolian sediment that may be derived from local and distant sources. OSL sensitivity tests were, therefore, applied to different grain-size fractions to investigate whether material may have been sourced from more freshly weathered or distant sources.

Sensitivity test were conducted using the SAR protocol and conditions described above. Aliquots were twice bleached at 20°C for 1000 s with a 10 000 s pause between bleaches. The response to a 50 Gy given dose (normalised by weight) was measured seven times. The first four measurements were conducted to measure initial sensitivity and change with dose cycle. Before the 5th measurement aliquots were heated to 500°C for 10 s and measured twice to assess the impact of

annealing. The final measurement was an IR-depletion point (Duller, 2003). Measurements were conducted on ten medium aliquots of 90–125 μm quartz (~2000 grains; Duller, 2008) and ten large aliquots 180–210 μm quartz (~1000 grains; Duller, 2008) of eight samples. Dune samples NAM07/3/2 and NAM07/4/12 from linear dunes of the Namib Sand Sea (see Stone *et al.*, 2010b for details) and NAM14/10/3 from dunes overlaying the Samara sand ramp were used as examples of aeolian material (assumed to undergone a number of cycles of sedimentation) from the region. These were compared with sand ramp body samples AUS13/1/1 (Aus), NAM14/1/2 (Rosh Pinah), NAM14/7/3 (Neuhof-1), NAM14/8/3 (Neuhof-2) and NAM14/12/1 (Sandkop).

Results

Sand ramp location and morphology

In total, 75 sand ramps were confirmed within the study region (Figure 2 and Supplementary information 2). 90% are climbing features as identified by their position in relation to topography and their morphology (Lancaster and Tchakerian, 1996; Chojnacki *et al.*, 2010; Goudie, 2013; Ellwein *et al.*, 2015). 74% are predominantly east facing and 17% are west facing (Figure 5 and Supplementary information 2). Accumulation occurs in sheltered alcoves or along elongate mountain fronts aligned perpendicular to the wind with 95% of sand ramps accumulated against inselbergs or inselberg complexes and 5% against the edge of the Great Escarpment (Supplementary

information 2 and Figure 5). All sand ramps are located either within 4 km of a large ephemeral river channel or within 5.5 km of a dune field (Supplementary information 2 and Figure 5).

Based on aerial morphology and field analysis, 33 sand ramps were classified as class 1, 23 as class 2, and 15 as class 3 (Supplementary information 2). As the identification of class 4 sand ramps requires sedimentary information, only Aus, Samara, Jagkop and an additional examined but unstudied sand ramp were grouped in this category (Supplementary information 2). The dunes overlaying the class 3 and 4 sands are perpendicular to the orientation of the sand ramp in 75% of the ramps and orientation is clearly modified by topography in 55% of cases.

Sand ramp sediments

Figure 6 depicts the sediment logs from the exposures and augured profiles within the sand ramps and from the overlaying dunes. Supplementary information 3 gives detailed sediment properties of the <2 mm size-fraction for samples within the sand-rich units.

A number of broad sediment characteristics are observed within the 10 sand ramps. These provide insight into depositional processes and are described as a series of 'units'. Unit 1 is the dominant sediment in the main bodies of all ten sand ramps. This is a matrix of moderately-well to poorly sorted medium sands with varying proportions of sub-rounded to angular gravels. This unit is split into loose unconsolidated sediments, found at the class 1–3 sand ramps (Unit 1(a)) and consolidated sediments observed at the class 3 and 4 sand ramps (Unit 1(b)), and suggests a dominance of aeolian sediments with minor components of gravel clasts provided by slope processes. Unit 2 represents situations where slope processes have dominated. Units comprise semi-continuous horizontal layers of cobble-sized material with occasional boulders, and are found interdigitated within the sediments at Aus (class 4), Jagkop (class 4), Samara (class 4) and Neuhof-1 (class 1) sand ramps. Unit 2 sediments are also found as a surface unit on parts of Aus (class 4), Jagkop (class 4), Samara (class 4), Neuhof-1 (class 1) Simplan (class 1) and Sandkop (class 3) ramps. Unit 3 comprises calcrete duricrust units, which are interpreted as pedogenic; these are found on the surface of class 4 ramps (Samara, Jagkop and Aus). There are less developed calcrete nodule layers found at depth within the Keerwader ramp. Unit 4 represents the purely aeolian sediments found in the dunes that overlay class 3 and class 4 sand ramps. This comprises moderately-well to poorly sorted medium sand without any larger clasts, which alongside the morphology of the features can be unambiguously assigned to aeolian deposition.

Sand ramp ages

Details of the luminescence ages are displayed in Table III. The 10 dated sand ramps indicate that sand ramp and dune accumulation in southern Namibia occurred episodically for >200 ka with the majority of dated activity occurring between ~80–12 ka (Figure 6). Holocene dates are mostly obtained from dunes, near surface sediments or slumped gullies. Material from the main body of class 1 and 2 sand ramps, and the overlying dunes on Klein Aus (class 3), Samara (class 4) and Aus (class 4) provide the simplest data to interpret. The remaining dataset contains three more complicated attributes which require further explanation.

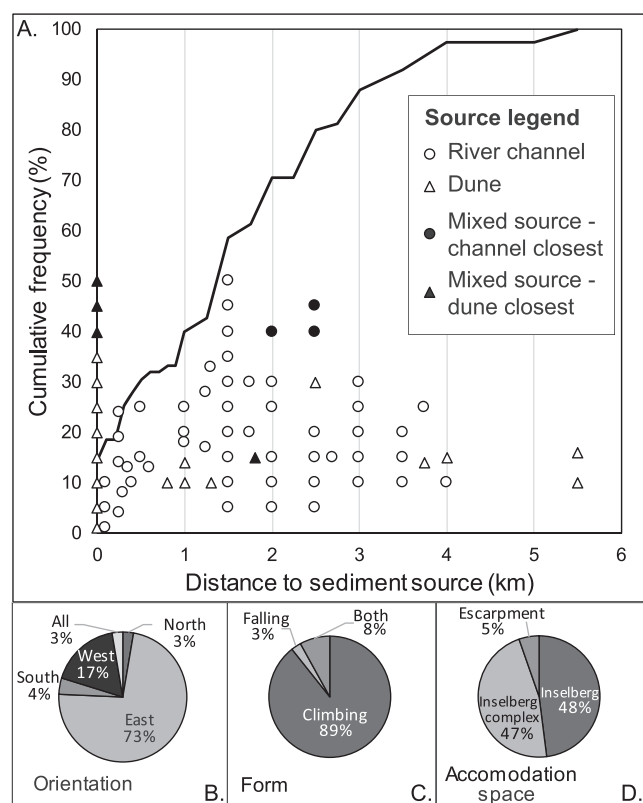


Figure 5. Properties of identified sand ramps. A). Distance to primary sediment source. Black line represents cumulative frequency by distance. Symbols depict the nature of the primary sediment source (circles = rivers, triangles = dunes), when both rivers and dunes provide possible sediment sources the symbol shape reflects the closest downwind source and symbols are opaque. B). Orientation of the sand ramp sediments (measured head to toe). C). Form of sand ramps. D). Type of accommodation space.

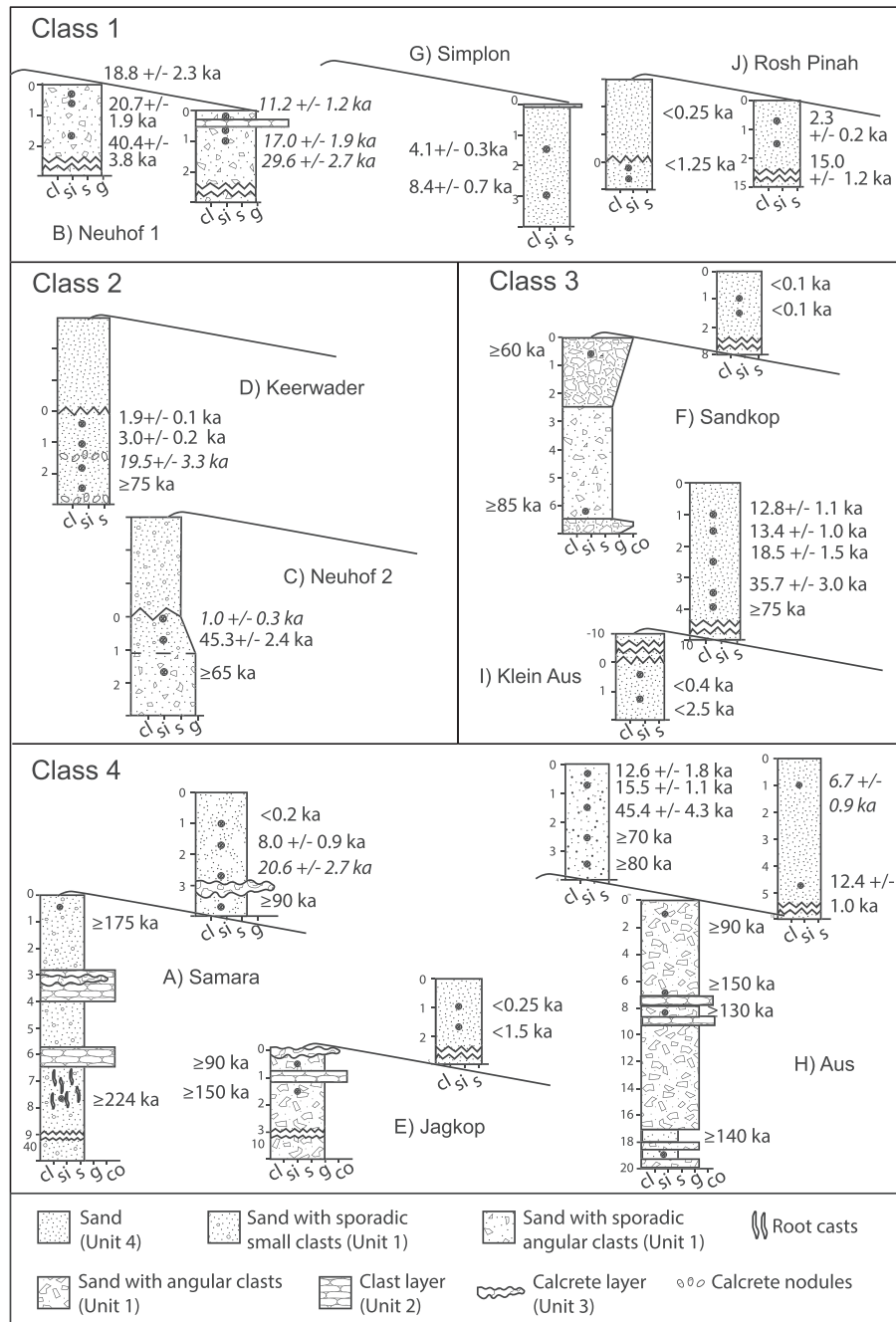


Figure 6. Schematic of sand ramp sediments and associated OSL ages, organised by class. Sloping black lines represent the sand ramp surface. Sediment logs positioned above this were taken from dunes overlaying the sand ramp sediments. Sediment logs positioned at the head of this line were taken from gullies at the head of the sand ramp and logs below the line in the centre were taken from gullies or pits in the centre of the sand ramp body. Width of the sediment logs represents maximum grain size (cl = clay, si = silt, s = sand, g = gravel, co = cobbles). Black circles indicate the position of OSL samples. Depth in meters is displayed on the y axis. For Neuhof-2 and Keerwader the marker above 0 represents the additional overburden of sediment which could not be sampled due to the gentle sloping side of the gully. In both cases this represents ~3m.

First, for some young samples ages were obtained from pilot studies of <10 aliquots. These are used to give indicative ages, and are displayed on Figure 6 as (< age). Pilot analysis of gully samples from Rosh Pinah (NAM13/1/1 and NAM13/1/2) and Klein Aus (NAM14/15/1 and NAM14/15/3) are younger than expected and show greater than expected scatter in D_e values indicating these sediments have been reworked, most likely due to slumping. Dune samples from Sandkop (NAM14/13/1 and NAM14/13/2) contained very high levels of feldspar contamination. Pilot studies indicated these samples were very young (<0.1 ka) but no further analysis was conducted.

Second, a number of gully and dune samples from class 2, 3 and 4 sand ramps are approaching luminescence saturation

(~200 Gy in this dataset). These ages are therefore quoted as minimum ages (> age).

Third, there are a number of samples with high (>30%) to very high (124%) overdispersion values that require interpretation alongside their field setting, and caution to be applied when their age estimates are considered. These ages are displayed in italics in Figure 6. 124% overdispersion in sample NAM14/8/1 (Neuhof-2) is linked to very high concentrations of plant roots in the sediment body from which the sample was taken. Therefore, overdispersion is most likely a result of bioturbation. 76% overdispersion in NAM14/5/3 (Keerwader) may result from beta microdosimetry caused by the calcrete nodules which surround this sample.

Relatively high overdispersion is also observed in Neuhoof-1 samples NAM14/7/1 (43%), NAM14/7/2 (34%) and NAM14/7/3 (32%) and Samara dune sample NAM14/10/3 (38%). This may be due to the heterogeneous nature of the Neuhoof-1 substrate and the position of NAM14/10/3 above a calcrete layer creating beta heterogeneity. For Aus dune sample AUS13/6/1 (overdispersion of 40%) very low luminescence sensitivity is a significant contributor to the observed scatter.

Relationship between age and sand ramp morphology

The oldest sediment ages were obtained from the sediments of class 4 sand ramps and indicate accumulation >200 ka. The main bodies of class 2 and 3 sand ramps, aside from Klein Aus, date to 12–>75 ka while all class 1 dates are younger than 40 ka (Figure 6). This suggests some relationship between sand ramp size and complexity with age but only to the extent that the two end members, class 4 and class 1, are the oldest and youngest features, respectively. However, as class 1 ages are derived from the top 2 m of sediment or from toe sediments their relative youth in comparison with class 2 and class 3 features may be a function of sampling strategy. The erroneously young ages obtained from the gullies of Klein Aus and Rosh Pinah are thought to be due to recent slumping as sediments at both these locations struggled to hold a face. Dates from Neuhoof-1 and Rosh Pinah (class 1) were obtained only from the top 2 m of sediment wherein they show some stratigraphic constancy with dates from class 2 and 3 sand ramps (Figure 6). Near surface sediments of most dunes (class 3 and 4) and sand ramp bodies (class 1 and 2) show activity within the last 2 ka (Figure 6).

Relationship between age and sand ramp stratigraphy

Duricrust layers (Unit 3) are associated with a hiatus in sedimentation of >~70 ka (Jagkop, Samara) and calcrete nodules at Keerwader are associated with a hiatus of 13–20 ka (Figure 6). Consolidated sediments (Unit 1a) were deposited >~90 ka. The chronological significance of stone layers (Unit 2) is site specific, at Jagkop and Samara clast layers could represent a long-term hiatus in deposition while at Neuhoof-1 the stone layer represents a maximum hiatus of 7 ka (~4 ka weighted mean). Unconsolidated sand ramp sediments (Units 1b and 4) are dated to between 0.2 and >75 ka with no clear relationship between sedimentary features and accumulation rate (Figure 6).

Sediment provenance

The results of heavy mineral analyses are displayed in Figure 7 and can be used to assess whether the aeolian components of sand ramp sediments are derived from local or far-travelled sources.

All Aus samples contain a high garnet concentration and a secondary amphibole component (Figure 7(B)). This matches the Mesoproterozoic rocks of the Namaqua Metamorphic Complex which outcrops in the Aus region and consist mainly of garnet/kyanite to garnet-sillimanite paragneisses with subordinate orthogneisses and amphibolites (Becker *et al.*, 2006). At Neuhoof, the sediments of Neuhoof-1

(NAM14/6/2, NAM14/7/3) and Neuhoof-2 (NAM14/8/3) and the ephemeral river channel at the base of Neuhoof-1 (NAM14/6/R) are similar, all dominated by a very high amphibole content and a lesser epidote content (Figure 7 (B)). This shows strong agreement with the Neuhoof Formation described in this area (Becker *et al.*, 2006). The presence of kyanite in NAM14/7/3 and NAM14/8/3 (Figure 7) suggests a significant contribution from locally exposed amphibole-facies metasediments. At Jagkop, dune (NAM14/4/2) and sand ramp (NAM14/3/2) sediments are similar but not identical. Both contain significant pyroxene suggesting an affinity to the sands of the Orange River and the Namib Sand Sea (Garzanti *et al.*, 2012) (Figure 7(B)). However, heavy mineral concentration is low and the significant presence of amphibole, garnet, epidote and ZTR is akin to the local Sinclair Group geology (Figure 7(B)). The absence of pyroxenes at Aus and Neuhoof indicates zero to negligible supply of sediment from the Namib Sand Sea (Garzanti *et al.*, 2012) (Figure 7(B)).

Comparison of sand ramp sediments with samples from the Namib Sand Sea and the major ephemeral rivers of southern Namibia (Garzanti *et al.*, 2012) using PCA analysis shows Neuhoof and Aus are distinct from each other and from the Namib Sand Sea and major river systems (Figure 7(C)). Neuhoof-1 and the associated channel are closely related, while Jagkop shows similarities with the Namib Sand Sea and the major ephemeral rivers (Figure 7(C)). Overall these results indicate a local origin for the sand ramp sediments and suggest that the river sediments at Neuhoof have contributed material to the sand ramp.

Luminescence sensitivity tests on Unit 1 sediments from five of the sand ramps provide some additional insights into the provenance and depositional processes associated with these sediments.

Aeolian reference samples (NAM07/3/2, NAM07/4/12 and NAM14/10/3) show negligible sensitivity change in both size fractions after heating to 500°C. This indicates they have been significantly sensitised in nature by repeated burial cycles (Moska and Murray, 2006; Pietsch *et al.*, 2008; Fitzsimmons *et al.*, 2010). However, these reference samples also highlight a likely artefact relating to grain size and aliquot dimensions. Following initial measurement, the 90–125 µm size fraction is more sensitive than the 180–210 µm fraction (Figure 8(a)). This is most likely a product of an absolute increase in the number of luminescing grains in the smaller size fraction as the use of different aliquot sizes was not quite sufficient to normalise the number of grains (medium aliquots of 90–125 µm size grains likely to contain ~2000 grains compared with ~1000 grains in large aliquots of 180–210 µm (Duller, 2008)). This artefact is common to both aeolian reference and sand ramp samples. Therefore, the magnitude of sensitivity difference between grain-sizes in the aeolian reference samples provides a baseline to compare with the sand ramp sample data.

The 180–210 µm fraction from the Aus sand ramp sample (AUS13/1/1) demonstrates a large increase in luminescence signal intensity following heating (Figure 8(B)). This may partly reflect the different provenance of Aus sediments and the aeolian reference samples (Sawakuchi *et al.*, 2011a, b, Figure 7), but also suggests that the sediment has undergone fewer luminescence dosing and bleaching cycles. The sensitivity change after heating of the 90–125 µm size fraction is far more subdued (Figure 8(B)). In addition, the 90–125 µm size fraction is an order of magnitude more sensitive than the 180–210 µm fraction when responding to a given dose of 50 Gy (Figure 8(A)). This is well above the baseline difference observed in aeolian samples (Figure 8(A)) and indicates a real difference in sensitivity between the size fractions.

Table III. Luminescence properties

Site	Context	Sample	Depth (m)	n	De	OD (%)	ICP-MS		
							U (ppm)	Th (ppm)	K (%)
A) Samara [class 4]	Head gully	NAM14/9/1	0.3	11	337.27 ± 27.85	24 ± 3	1.01 ± 0.16	3.58 ± 0.72	1.27 ± 0.11
	Head gully	NAM14/9/2	7.8	11	331.5 ± 19.15	15 ± 2	0.8 ± 0.14	3.55 ± 0.48	1.01 ± 0.10
	O dunes	NAM14/10/1	1	7	0.19 ± 0.02	23 ± 3	0.89 ± 0.14	3.52 ± 0.70	1.17 ± 0.11
	O dunes	NAM14/10/2	1.8	20	19.22 ± 0.86	19 ± 1	0.5 ± 0.08	2.11 ± 0.42	1.69 ± 0.15
	O dunes	NAM14/10/3	2.8	20	36.47 ± 2.88	38 ± 4	0.87 ± 0.13	3.52 ± 0.70	1.22 ± 0.11
B) Neuhof 1 [class 1]	O dunes	NAM14/11/1	3.4	23	184.6 ± 19.62	42 ± 5	0.79 ± 0.12	3.44 ± 0.28	1.52 ± 0.06
	Main body	NAM14/6/1	0.4	18	56.49 ± 2.26	14 ± 1	1.8 ± 0.28	4.62 ± 0.92	1.73 ± 0.16
	Main body	NAM14/6/2	0.7	19	73.16 ± 5.99	25 ± 3	1.88 ± 0.29	6.05 ± 1.21	2.59 ± 0.23
	Main body	NAM14/6/3	1.8	14	152.35 ± 10.75	23 ± 3	1.75 ± 0.27	10.32 ± 2.06	2.61 ± 0.24
	Main body	NAM14/7/1	0.25	27	42.84 ± 2.26	43 ± 4	2.18 ± 0.34	10.09 ± 2.02	2.50 ± 0.22
C) Neuhof 2 [class 2]	Main body	NAM14/7/2	0.6	12	66.29 ± 6.79	34 ± 4	2.17 ± 0.16	8.19 ± 0.2	2.79 ± 0.15
	Main body	NAM14/7/3	1	26	101.77 ± 6.91	32 ± 3	1.85 ± 0.29	6.3 ± 1.26	2.51 ± 0.23
	Head gully	NAM14/8/1	0.15	26	3.83 ± 0.90	124 ± 19	1.5 ± 0.23	5.41 ± 1.08	3.00 ± 0.27
	Head gully	NAM14/8/2	0.8	15	177.39 ± 7.81	13 ± 1	1.46 ± 0.03	4.72 ± 0.3	3.27 ± 0.01
	Head gully	NAM14/8/3	1.6	20	221 ± 11.72	19 ± 2	1.52 ± 0.24	5.46 ± 1.09	2.54 ± 0.23
D) Keerwader [class 2]	Head gully	NAM14/5/1	0.5	27	6.58 ± 0.13	9 ± 1	1.81 ± 0.28	6.72 ± 1.34	2.40 ± 0.22
	Head gully	NAM14/5/2	1.1	16	8.46 ± 0.41	19 ± 2	1.86 ± 0.29	6.34 ± 1.27	1.89 ± 0.17
	Head gully	NAM14/5/3	1.8	23	72.5 ± 11.58	76 ± 10	1.56 ± 0.24	7.46 ± 1.49	2.80 ± 0.25
	Head gully	NAM14/5/4	2.5	10	301.86 ± 34.25	32 ± 5	1.54 ± 0.27	7.33 ± 3.63	3.09 ± 0.14
E) Jagkop [class 4]	Head gully	NAM13/3/1	0.4	7	311.4 ± 41.27	33 ± 6	2.55 ± 0.40	6.6 ± 1.32	2.00 ± 0.18
	Head gully	NAM13/3/3	1.9	7	249.22 ± 53.41	55 ± 12	0.98 ± 0.15	3.48 ± 0.70	1.04 ± 0.09
	O dunes	NAM13/4/1	1	4	0.46 ± 0.16	-	1.18 ± 0.18	5.63 ± 1.13	2.81 ± 0.25
	O dunes	NAM13/4/2	1.8	4	4.87 ± 0.06	-	1.34 ± 0.21	5.14 ± 1.03	2.69 ± 0.24
F) Sandkop [class 3]	Head gully	NAM14/12/1	0.5	22	219.37 ± 14.09	27 ± 2	1.23 ± 0.19	10.08 ± 2.02	2.14 ± 0.19
	Head gully	NAM14/12/7	6.2	25	288.14 ± 17.74	29 ± 2	1.18 ± 0.09	9.25 ± 0.80	2.35 ± 0.30
	O dunes	NAM14/13/1	1	4*	0.08 ± 0.04	-	0.8 ± 0.12	5.66 ± 1.13	2.20 ± 0.20
	O dunes	NAM14/13/2	1.5	4*	0.1 ± 0.03	-	0.96 ± 0.15	6.11 ± 1.22	2.20 ± 0.20
G) Simplon [class 1]	Main body	AUS13/7/1	1.5	23	7.38 ± 0.46	28 ± 2	1.27 ± 0.20	5.46 ± 1.09	1.02 ± 0.09
	Main body	AUS13/7/2	3	24	15.39 ± 0.50	15 ± 1	1.35 ± 0.21	5.48 ± 1.10	1.05 ± 0.09
H) Aus [class 4]	Main body	AUS13/1/1	2	17	505.11 ± 34.24	24 ± 3	1.34 ± 0.21	10.27 ± 2.05	3.42 ± 0.31
	Main body	AUS13/1/4	8	6	629.48 ± 49.62	4 ± 2	1.95 ± 0.30	14.37 ± 2.87	2.74 ± 0.25
	Main body	AUS13/1/6	9.2	5	559.3 ± 78.35	27 ± 6	2.24 ± 0.35	15.94 ± 3.19	2.77 ± 0.25
	Main body	AUS13/1/11	19.7	9	531.6 ± 21.85	22 ± 1	1.8 ± 0.28	12.43 ± 2.49	2.59 ± 0.23
	O dunes	AUS13/3/1	0.35	31	64.08 ± 8.15	67 ± 7	2.6 ± 0.40	18.97 ± 3.79	3.13 ± 0.28
	O dunes	AUS13/3/2	0.7	47	90.02 ± 4.74	29 ± 2	3.38 ± 0.52	23.21 ± 4.64	3.15 ± 0.28
	O dunes	AUS13/3/3	1.5	22	247.31 ± 16.66	29 ± 3	2.84 ± 0.44	23.65 ± 4.73	3.17 ± 0.29
	O dunes	AUS13/3/4	2.5	9	344.86 ± 19.91	15 ± 2	2.37 ± 0.37	15.75 ± 3.15	2.97 ± 0.27
	O dunes	AUS13/3/5	3.5	18	323.12 ± 12.96	8 ± 2	1.57 ± 0.08	10.73 ± 1.5	2.95 ± 0.05
	Toe dunes	AUS13/6/1	1	11	38.58 ± 4.76	40 ± 6	2.75 ± 0.43	23.94 ± 4.79	3.52 ± 0.32
	Toe dunes	AUS13/6/5	4.7	14	65.31 ± 3.38	12 ± 12	2.56 ± 0.40	19.56 ± 3.91	3.34 ± 0.30
	O dunes	NAM14/14/1	1	25	52.41 ± 3.28	22 ± 2	1.79 ± 0.28	10.34 ± 2.07	2.86 ± 0.26
I) Klein Aus [class 3]	O dunes	NAM14/14/2	1.5	24	72.83 ± 2.71	16 ± 1	2.66 ± 0.41	16.39 ± 3.28	3.72 ± 0.33
	O dunes	NAM14/14/3	2.5	23	98.13 ± 5.12	24 ± 2	2.57 ± 0.40	16.39 ± 3.28	3.61 ± 0.33
	O dunes	NAM14/14/4	3.5	22	196.8 ± 11.22	24 ± 2	2.92 ± 0.45	17.84 ± 3.57	3.66 ± 0.33
	O dunes	NAM14/14/5	4	10	345.2 ± 20.90	11 ± 2	2.33 ± 0.36	13.83 ± 2.77	2.90 ± 0.26
	Head Gully	NAM14/15/1	0.5	4	0.92 ± 0.59	-	0.78 ± 0.12	3.41 ± 0.68	3.34 ± 0.30
J) Rosh Pinah [class 1]	Head Gully	NAM14/15/3	1.3	4	4.78 ± 4.67	-	1.42 ± 0.22	7.83 ± 1.57	3.18 ± 0.29
	Side Gully	NAM14/1/1	0.4	4	0.43 ± 0.07	-	0.79 ± 0.12	2.75 ± 0.55	1.41 ± 0.13
	Side Gully	NAM14/1/2	0.8	4	2.24 ± 0.60	-	1.22 ± 0.19	5.94 ± 1.19	1.41 ± 0.13
	Main body	NAM14/2/1	0.9	23	4.98 ± 0.16	12 ± 1	1.16 ± 0.18	4.90 ± 0.98	1.43 ± 0.13
	Main body	NAM14/2/2	1.5	23	37.26 ± 1.10	14 ± 1	1.3 ± 0.20	6.05 ± 1.38	1.67 ± 0.20

Ages calculated using CAM (Galbraith, 1999). n = number of accepted aliquots, OD = Overdispersion

*(All aliquots of NAM14/13/1 & NAM14/13/2 failed the IR-depletion ratio significantly)

A notable sensitivity change after heating to 500°C is also observed in the 180–210 µm size fraction of the Sandkop sample (NAM14/12/1) with some difference in sensitivity between the grainsizes also observed (Figure 8). The observations from other sand ramps are less conclusive. This preliminary dataset highlights the potential of this technique as a provenancing tool but also demonstrates the variability of sand ramp sediments and the need for a larger dataset before definitive conclusions can be drawn for all sand ramps.

Discussion

Controls on sand ramp formation

Data on the locations and sediments of confirmed sand ramps (Figure 2, Figure 5) indicate that four factors govern sand ramp formation in southern Namibia:

1. an adequate supply of sediment with significant aeolian transport potential;
2. an appropriate accommodation space;
3. directionally-persistent winds with sufficient energy for aeolian sand transport;
4. an arid to semi-arid climate but with sufficient seasonal, or longer term, variability to promote differing geomorphic and depositional processes.

All four factors need to be met for sand ramp accumulation to occur (Figure 9). Factors 1 and 2 are local and determine where sand ramps form in a region where factors 3 and 4 are met. Within southern Namibia the bimodal wind direction and local perturbations of factor 3 also have a local influence on the distribution of sand ramps. Therefore, the pattern of sand ramp (non) occurrence in southern Namibia can be explained by factors 1, 2 and 3 (Figure 9).

All sand ramps are within 5.5 km downwind of sand sources in the form of river channels or dune fields (Supplementary information 2

Table III. (continued)

Site	Gamma spectrometry			Beta dose (Gy/ka)	Gamma dose (Gy/ka)	Cosmic dose (Gy/ka)	Dose rate (Gy/ka)	Age (ka)	Quoted age (ka)
	U (ppm)	Th (ppm)	K (%)						
A) Samara	-	-	-	1.11 ± 0.10	0.57 ± 0.05	0.26 ± 0.03	1.94 ± 0.20	173.49 ± 22.75	≥170
[class 4]	-	-	-	0.89 ± 0.08	0.48 ± 0.04	0.10 ± 0.01	1.48 ± 0.09	224.44 ± 19.07	≥225
	-	-	-	1.02 ± 0.09	0.53 ± 0.05	0.21 ± 0.02	1.77 ± 0.18	0.11 ± 0.02	<0.2
	-	-	-	1.33 ± 0.12	0.55 ± 0.05	0.19 ± 0.02	2.42 ± 0.26	7.95 ± 0.93	
	-	-	-	1.06 ± 0.09	0.54 ± 0.05	0.17 ± 0.02	1.77 ± 0.19	20.64 ± 2.73	
	-	-	-	1.26 ± 0.07	0.60 ± 0.03	0.16 ± 0.02	2.02 ± 0.08	91.34 ± 10.30	≥90
B) Neuhoof 1	-	-	-	1.56 ± 0.13	0.81 ± 0.07	0.25 ± 0.03	3.00 ± 0.35	18.84 ± 2.31	
[class 1]	1.79 ± 0.25	8.89 ± 0.68	2.07 ± 0.16	2.22 ± 0.19	1.17 ± 0.07	0.22 ± 0.02	3.61 ± 0.21	20.73 ± 1.86	
	-	-	-	2.31 ± 0.20	1.27 ± 0.12	0.19 ± 0.02	3.77 ± 0.23	40.43 ± 3.79	
	-	-	-	2.27 ± 0.19	1.28 ± 0.12	0.26 ± 0.03	3.81 ± 0.23	11.19 ± 1.23	
	2.54 ± 0.32	10.22 ± 0.78	2.14 ± 0.17	2.44 ± 0.14	1.32 ± 0.08	0.23 ± 0.02	3.99 ± 0.17	16.95 ± 1.87	
	-	-	-	2.16 ± 0.19	1.08 ± 0.09	0.21 ± 0.02	3.44 ± 0.21	29.57 ± 2.69	
C) Neuhoof 2	-	-	-	2.46 ± 0.22	1.11 ± 0.09	0.29 ± 0.03	3.86 ± 0.42	0.98 ± 0.26	
[class 2]	1.52 ± 0.19	6.04 ± 0.47	2.66 ± 0.20	2.64 ± 0.10	1.20 ± 0.08	0.22 ± 0.02	4.05 ± 0.13	45.32 ± 2.42	
	-	-	-	2.13 ± 0.19	1.01 ± 0.09	0.19 ± 0.02	3.33 ± 0.21	66.41 ± 5.41	≥65
D) Keerwader	-	-	-	2.09 ± 0.18	1.07 ± 0.09	0.24 ± 0.02	3.39 ± 0.20	1.95 ± 0.12	
[class 2]	-	-	-	1.72 ± 0.15	0.93 ± 0.08	0.21 ± 0.02	2.86 ± 0.17	2.96 ± 0.23	
	-	-	-	2.36 ± 0.21	1.17 ± 0.10	0.19 ± 0.02	3.71 ± 0.23	19.53 ± 3.35	
	1.50 ± 0.21	6.57 ± 0.53	2.66 ± 0.20	2.56 ± 0.16	1.21 ± 0.08	0.17 ± 0.02	3.95 ± 0.18	78.96 ± 9.65	≥75
E) Jagkop	2.04 ± 0.26	8.35 ± 0.64	1.84 ± 0.15	1.88 ± 0.16	1.10 ± 0.07	0.26 ± 0.03	3.41 ± 0.17	99.5 ± 14.28	≥100
[class 4]	-	-	-	0.94 ± 0.08	0.51 ± 0.05	0.22 ± 0.02	1.67 ± 0.09	149.59 ± 33.15	≥150
	-	-	-	2.29 ± 0.20	1.04 ± 0.09	0.21 ± 0.02	3.54 ± 0.22	0.13 ± 0.05	<0.25
	-	-	-	2.21 ± 0.20	1.01 ± 0.09	0.19 ± 0.02	3.41 ± 0.21	1.43 ± 0.20	<1.5
F) Sandkop	1.87 ± 0.32	13.43 ± 1.01	2.29 ± 0.18	1.90 ± 0.16	1.37 ± 0.09	0.25 ± 0.03	3.52 ± 0.19	62.67 ± 5.24	≥60
[class 3]	1.71 ± 0.86	11.29 ± 0.86	2.26 ± 0.18	2.03 ± 0.23	1.32 ± 0.08	0.12 ± 0.01	3.87 ± 0.24	85.24 ± 8.33	≥85
	-	-	-	1.80 ± 0.16	0.86 ± 0.08	0.22 ± 0.02	2.88 ± 0.18	0.03 ± 0.01	<0.1
	-	-	-	1.83 ± 0.16	0.90 ± 0.08	0.21 ± 0.02	2.94 ± 0.18	0.03 ± 0.01	<0.1
G) Simplan	-	-	-	1.00 ± 0.08	0.62 ± 0.06	0.20 ± 0.02	1.82 ± 0.11	4.06 ± 0.35	
[class 1]	-	-	-	1.03 ± 0.09	0.64 ± 0.06	0.16 ± 0.02	1.83 ± 0.11	8.41 ± 0.56	
H) Aus	2.76 ± 0.40	18.77 ± 1.40	2.91 ± 0.23	2.84 ± 0.25	1.93 ± 0.12	0.19 ± 0.02	4.96 ± 0.28	90.00 ± 7.72	≥90
[class 4]	-	-	-	2.51 ± 0.21	1.51 ± 0.16	0.10 ± 0.01	4.12 ± 0.5	153.05 ± 22.27	≥150
	-	-	-	2.54 ± 0.21	1.62 ± 0.17	0.09 ± 0.10	4.24 ± 0.27	131.79 ± 20.31	≥130
	-	-	-	2.34 ± 0.20	1.37 ± 0.14	0.04 ± 0.00	3.75 ± 0.24	141.80 ± 10.85	≥140
	-	-	-	2.96 ± 0.25	1.88 ± 0.20	0.26 ± 0.03	5.09 ± 0.32	12.57 ± 1.76	
	3.99 ± 0.54	25.18 ± 1.87	2.82 ± 0.23	3.15 ± 0.26	2.29 ± 0.14	0.23 ± 0.02	5.66 ± 0.03	15.50 ± 1.09	
	-	-	-	3.12 ± 0.26	2.13 ± 0.24	0.20 ± 0.02	5.44 ± 0.36	45.44 ± 4.27	≥45
	-	-	-	2.75 ± 0.23	1.67 ± 0.17	0.18 ± 0.02	4.60 ± 0.29	74.96 ± 6.35	≥75
	-	-	-	2.54 ± 0.10	1.35 ± 0.08	0.16 ± 0.02	4.05 ± 0.13	79.76 ± 4.15	≥80
	-	-	-	3.36 ± 0.28	2.21 ± 0.25	0.21 ± 0.02	5.78 ± 0.38	6.67 ± 0.93	
	-	-	-	3.12 ± 0.26	1.95 ± 0.21	0.14 ± 0.01	5.21 ± 0.34	12.49 ± 0.98	
I) Klein Aus	-	-	-	2.49 ± 0.21	1.34 ± 0.12	0.22 ± 0.02	4.05 ± 0.25	12.84 ± 1.08	
[class 3]	-	-	-	3.34 ± 0.28	1.91 ± 0.19	0.21 ± 0.02	5.45 ± 0.34	13.36 ± 0.97	
	-	-	-	3.25 ± 0.28	1.87 ± 0.18	0.18 ± 0.02	5.31 ± 0.33	18.50 ± 1.51	
	-	-	-	3.36 ± 0.28	1.99 ± 0.20	0.16 ± 0.02	5.51 ± 0.35	35.74 ± 3.03	≥35
	-	-	-	2.66 ± 0.22	1.56 ± 0.15	0.15 ± 0.02	4.37 ± 0.27	79.01 ± 6.87	≥75
	-	-	-	2.58 ± 0.24	1.03 ± 0.09	0.25 ± 0.03	3.86 ± 0.26	0.24 ± 0.15	<0.4
	-	-	-	2.63 ± 0.23	1.26 ± 0.11	0.21 ± 0.02	4.10 ± 0.26	1.17 ± 1.14	<2.5
	-	-	-	1.17 ± 0.10	0.54 ± 0.05	0.22 ± 0.02	1.93 ± 0.12	0.22 ± 0.04	<0.25
J) Rosh Pinah	-	-	-	1.29 ± 0.11	0.86 ± 0.05	0.19 ± 0.02	2.34 ± 0.12	0.98 ± 0.26	<1.25
[class 1]	1.36 ± 0.20	6.97 ± 0.54	1.45 ± 0.11	1.27 ± 0.11	0.68 ± 0.06	0.19 ± 0.02	2.15 ± 0.13	2.32 ± 0.16	
	-	-	-	1.48 ± 0.16	0.81 ± 0.09	0.18 ± 0.02	2.47 ± 0.18	15.00 ± 1.19	

Ages calculated using CAM (Galbraith, 1999). n = number of accepted aliquots, OD = Overdispersion

*(All aliquots of NAM14/13/1 & NAM14/13/2 failed the IR ratio significantly)

and Figure 5). Heavy mineral analysis indicates the sediments of the Aus, Neuhoof-1, Neuhoof-2 and to some extent Jagkop sand ramps are sourced from the local geology (Figure 7). The Jagkop sand ramp sediment also shows some affinity with the Namib Sand Sea, reflecting its location on the margin of the the Namib Sand Sea. For the Neuhoof sand ramps the affinity to the local stream indicates that this is a potential sediment source (Figure 7).

Ramps do not accumulate against larger mountain complexes with significant run-off generation or when there are no sheltered accommodation spaces perpendicular to the wind (Figure 9). Thus, suitable accommodation spaces must be subject to minimal aeolian and alluvial erosion. Typically, these are small concave facets on inselbergs/small inselberg complexes or along the flanks of elongate inselbergs (Supplementary information 2, Figure 2). Local topographic perturbations in wind dynamics influence aeolian transport

potential (Xianwan *et al.*, 1999) and thus sand ramps do not form in accommodation spaces where winds are disrupted by topographic obstacles, despite the occurrence of available sediment sources (Supplementary information 2 and Figure 2, Figure 9).

Over 70% of sand ramps in this study are east-facing. All of these ramps are climbing features and all morphological classes are represented. >80% of west-facing sand ramps are small, class 1 features and ~10% are falling features. West-facing class 3 or 4 ramps are not observed (Supplementary information 2 and Figure 5). This suggests that seasonal easterly winds are the primary creator of sand ramps in southern Namibia while the prevailing SW winds also have a small influence. Wind measurements are sparse on the eastern margin of the Namib Sand Sea (Livingstone *et al.*, 2010). Nevertheless, available data agree with the distribution of sand ramps. SW winds are capable of reaching transport velocities

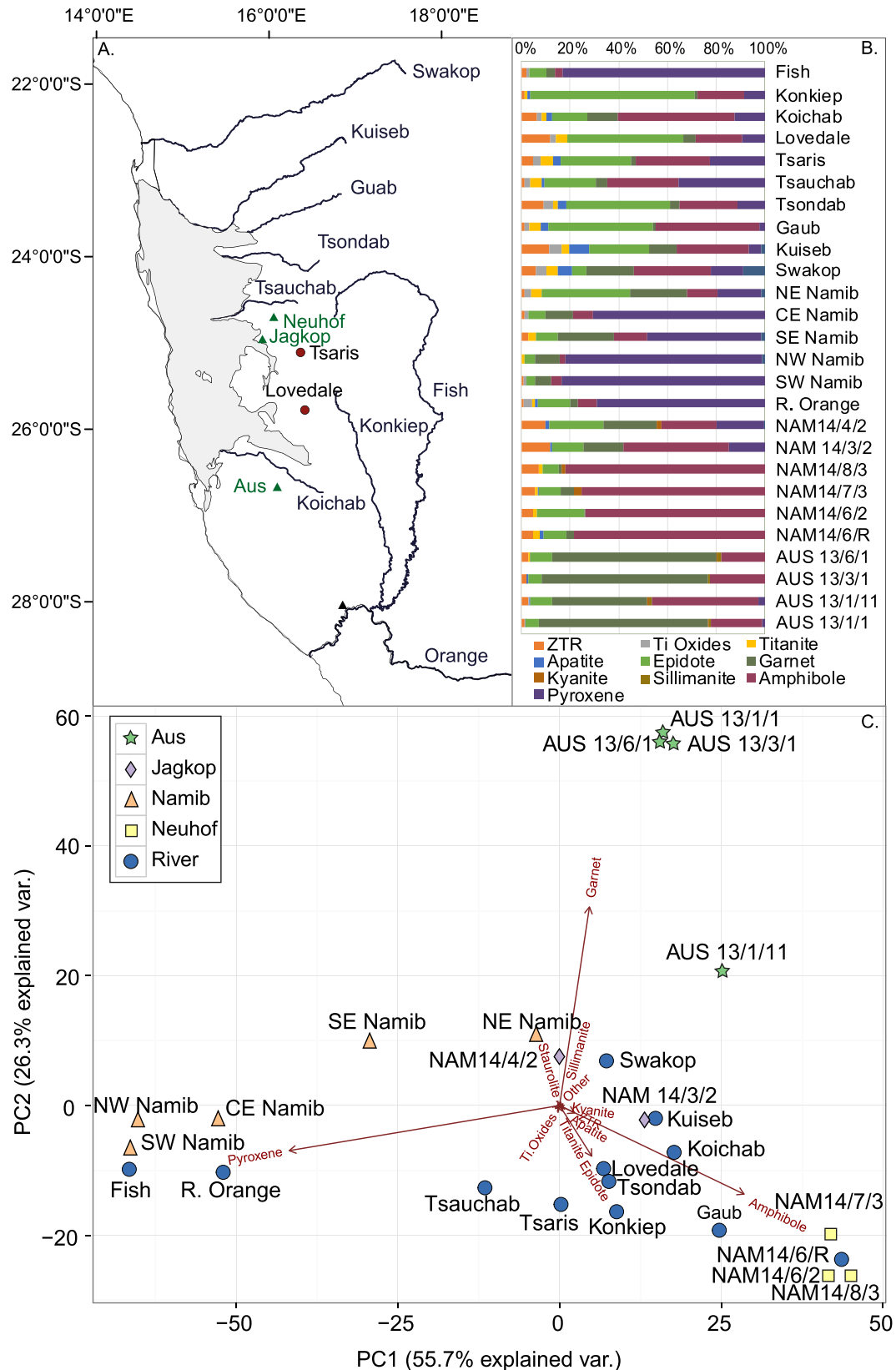


Figure 7. Heavy mineral properties of Aus sand ramp (AUS13/1/1, AUS13/1/11) and dunes (AUS13/3/1, AUS13/6/1), Neuhoef-2 sand ramp (NAM14/8/3), Neuhoef-1 sand ramp (NAM14/6/2, NAM14/7/3) and associated ephemeral river channel (NAM14/6/R), Jagkop sand ramp (NAM14/3/2) and dunes (NAM14/4/2) in comparison to major ephemeral rivers of southern Namibia and dunes of the Namib Desert (data from Garzanti *et al.*, 2012). (A). Sampling locations. Rivers were sampled at multiple locations along their course (see Garzanti *et al.* 2012). (B). Heavy mineral composition by percent. (C). Biplot of heavy mineral PCA results Component 1 is primarily controlled by the difference between amphibole and pyroxene and explains 56% of the variance. Component 2 is controlled by the contrast between garnet, and amphibole, epidote and pyroxene apatite and explains 26% of variance. Proximity of samples to vectors or each other indicates similarity. [Colour figure can be viewed at wileyonlinelibrary.com]

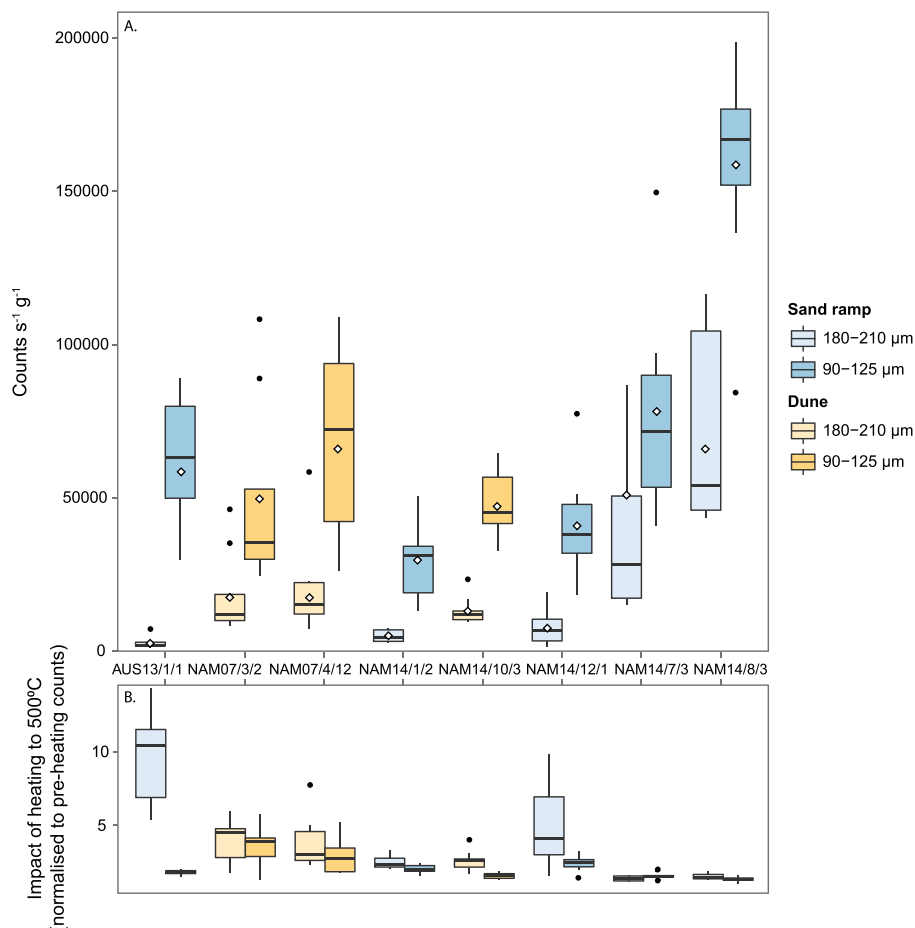


Figure 8. Luminescence sensitivity of different grain-sizes (A.) in response to a 50 Gy given dose (B) in response to a 50 Gy given dose after heating to 500°C (normalised to pre-heating counts/s/g). Box plots show the interquartile range, outliers are shown by black dots. Black lines represent the median and white diamonds the mean. [Colour figure can be viewed at wileyonlinelibrary.com]

~2% of the time but wind speeds rarely exceed 8 m s^{-1} . Easterly winds only reach transport velocities ~0.5% of the time but can reach speeds of $14\text{--}17 \text{ m s}^{-1}$ and thus total sand transport potential is greater (Lancaster *et al.*, 1984; Lancaster, 1985). Satellite imagery indicates that there are several west facing accommodation spaces that currently do not contain sand ramps (Figure 9).

Timescale of sand ramp accumulation

OSL dates confirm provisional dating by Bertram (2003) and indicate that sand ramps have been present in the Namibian landscape for over 100 ka (Figure 6). This demonstrates that sand ramps are not solely features of the Last Glacial and that they can act as long-term sediment stores. Akin to Telfer *et al.* (2012) and Ellwein *et al.* (2015) deposition is episodic for most ramps with only Simplon (class 1) potentially representing a single, rapid phase of deposition as described by Bateman *et al.* (2012) and Thomas *et al.* (1997) (Figure 6). Chronologies vary between sand ramps reflecting local accommodation space availability, sediment supply and wind dynamics but common periods of activity are apparent (Figure 6).

Significance of sand ramp morphology

There is some relationship between sand ramp morphological class and age but only to the extent that the large and sedimentologically complex class 4 sand ramps are of greatest antiquity while younger ages are found from the smallest, class 1

features (Figure 6). However, basal head-gully dates are not available for the class 1 sand ramps so a true comparison with other classes cannot be made. The lack of a clear relationship between morphology and age indicates that sand ramps do not follow a common evolution of increasing size and complexity over time and therefore, aside from the class 4 sand ramps with significant duricrust formation, morphological class cannot be used as a predictor of age. Instead, the size and morphological complexity of the sand ramp is more likely to be determined by the size and shape of the accommodation space.

Akin to the sand ramps in this study, large free-form dunes are frequently superimposed by smaller dunes (Lancaster, 2009; Livingstone *et al.*, 2010). The mechanism controlling superimposition is debated with large-scale changes in wind regime and climate (Warren and Allison, 1998), seasonal or annual variation in wind (Bristow *et al.*, 2007), landscape patterning and self-organisation (Ewing *et al.*, 2006; Dong *et al.*, 2009) and stabilisation of the underlying dune due to climatic change (Dong *et al.*, 2004) all suggested as potential drivers. There is some evidence that the size of the dune determines the quantity and complexity of superimposed features with secondary features unable to form where the primary dune is below a certain size (Breed and Grow, 1979; Al-Masrahy and Mountney, 2013). Thus, secondary dunes may simply be a function of airflow fluctuation created when the flanks of the dunes are large enough to form a planar surface (Lancaster, 1988). In this study superimposed dunes only form on sand ramps with a length or width $> 1 \text{ km}$ with the number of secondary features increasing with sand ramp size (Supplementary information 2). Therefore, for these sand

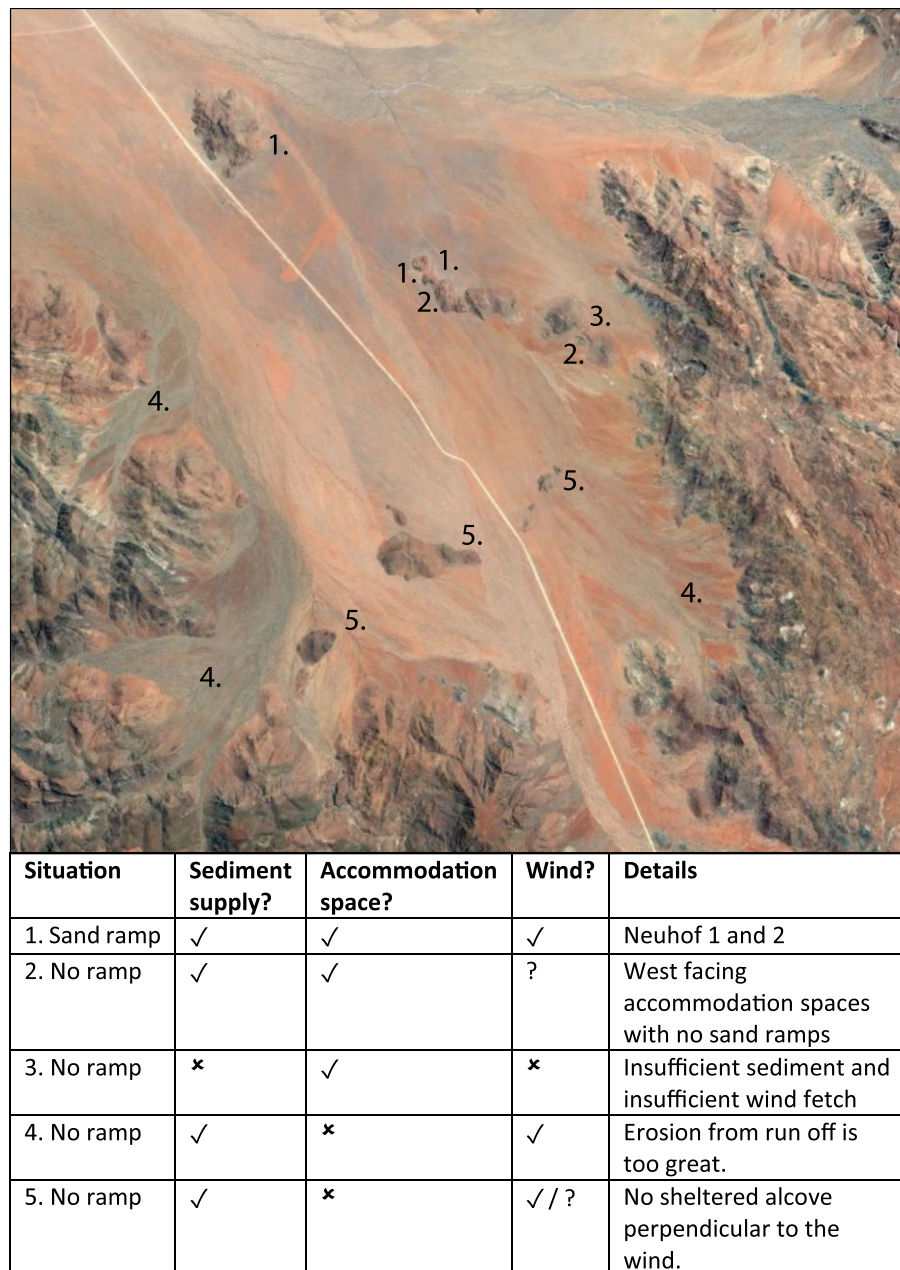


Figure 9. Real world example of the controls on sand ramp location. (A) Numbers characterise potential accommodation spaces within an ephemeral river valley. (B) The corresponding (non-)presence of sand ramps is explained based on the factors controlling sand ramp location. [Colour figure can be viewed at wileyonlinelibrary.com]

ramps, superimposed dune features are likely to represent the opportunistic filling of the secondary accommodation space created by the planar flank of the ramp.

The main bodies of the sampled class 3 and 4 sand ramps are semi-consolidated to consolidated (Unit 1b) and date to >60 ka. The superimposed dunes of class 3 and 4 ramps (Unit 4) and the main bodies of class 1 and 2 ramps are unconsolidated (Unit 1a) and have episodic chronologies from present to >75 ka (Figure 6). This suggests that after sand ramps reach a certain size (~1 km in length or width in this study) aeolian deposition becomes focused on the superimposed dunes, enabling the underlying sand ramp sediments to stabilize. Therefore, class 3 and 4 ramps may preserve initial accumulation with little reworking. The small size of class 1 and 2 sand ramps inhibits the formation of secondary features and thus, unless protected by a talus mantle, surface sediments are vulnerable to aeolian reworking. The parallels between dune and class 1 and 2 chronologies (Figure 6) suggests both are responding to the same environmental forcing. In this way, the size of the

accommodation space, and thus the size of the sand ramp, controls the accumulation history of the sand ramp.

Accommodation space may also control the formation of the gullies which separate the head of sand ramps from topographic obstacles. Steep slopes promote reverse flow and thus aeolian erosion (Tsoar, 1983; Pye and Tsoar, 1990; Qian *et al.*, 2011a, b) while the accommodation space also channels run-off to promote either continued erosion downslope or erosion at the head of the sand ramp. All gullies now show evidence of flow and fluvial erosion but, depending on the accommodation space, aeolian activity may have played a role in initiation at some sites.

Gullies at the head of the sand ramps protect the sediments from downslope fluvial erosion but also provide a mechanism for sediment to be removed from the sand ramp via aeolian erosion and slumping. This is exemplified by the erroneously young ages obtained from the gully of Klein Aus and from the shallow gully of Rosh Pinah (Figure 5). Therefore, if gullies have been present throughout sand ramp accumulation, episodic

deposition at Keerwader and Neuhof-2 may be explained by repeated periods of aeolian erosion and subsequent accommodation space availability and accumulation. This may explain some correspondence between the dune and sand ramp records.

Significance of sedimentary features

The consolidation of sediments (Unit 1b) and the formation of duricrust layers (Unit 3) is associated with sand ramp stability while the significance of stone layers and the chronology of unconsolidated sediments is site specific (Figure 6). Well-developed calcretes (such as those at Samara, Jagkop and Aus) require lengthy development times under stable conditions with little sediment input (Wright, 2007). At Samara, calcrete formation is associated with a ~70 ka hiatus in accumulation while ages from consolidated sediments below duricrusts at Aus and Jagkop are >100 ka indicating long-term sand ramp stability. Calcretes increase in complexity with time (Netterberg, 1969). Simple calcrete nodules at Keerwader are associated with a 13–20 ka hiatus, indicating medium term stability. Akin to Bateman *et al.* (2012) and Rendell and Sheffer (1996) buried stone layers (Unit 2) are not always associated with long accumulation hiatuses. At Neuhof-1 the stone layer represents between c.1.6 and 7.1 ka (mean 4.3 ka) possibly suggesting event driven distribution (*cf* Bateman *et al.*, 2012) while a longer period of stability is possible for Jagkop (Figure 6). Unconsolidated sand ramp sediments (Unit 1a) do not necessarily represent recent activity with ages ranging between 0.2 and >75 ka with no clear relationship between sedimentary features and chronology.

Palaeoenvironmental significance of sand ramps

Due to the number of geomorphic processes operating on sand ramps, accumulation is unlikely to be a binary process of solely aeolian or solely colluvial deposition followed by preservation. This is typified by unit 1 which indicates a mix of both aeolian and colluvial processes operating within the same unit. In addition, the difference in luminescence sensitivity between size fractions of AUS13/1/1 suggests that the 90–125 μm fraction has undergone several charge accumulation and bleaching cycles (i.e. an aeolian sediment history) before being deposited while the 180–210 μm fraction is more likely to be freshly weathered material (i.e. colluvium) (Moska and Murray, 2006; Pietsch *et al.*, 2008; Fitzsimmons *et al.*, 2010). The presence of both populations in a single sample indicates interplay between the two depositional mechanisms. This is supported by the poor sorting of the <2 mm fraction, the presence of angular clasts among the aeolian sands and the frequent absence of bedding structures in aeolian units (Lancaster and Tchakerian, 1996; Bertram, 2003).

Akin to the sand ramps of the Mojave (Pease and Tchakerian, 2003), sediment supply to the Aus and Neuhof sand ramps is of local origin with the heavy mineral assemblages reflecting the local lithology (Figure 7, Becker *et al.*, 2006). At Neuhof-1 the heavy mineral suite from the sand ramp and the neighbouring ephemeral river channel are nearly identical, confirming the potential of the river channel as a sediment source. At Jagkop the heavy mineral assemblage closely resembles the local lithology but with 15–30% contribution from the dunes of the Namib Sand Sea which are immediately to the south and east of the mountain. All sand ramps studied are within 4 km of river channels or within 5.5 km of dune

fields (Figure 5), suggesting these are the most likely sediment sources. The local origin of the sediments suggests that periods of colluvial and aeolian deposition both reflect local environmental conditions and if the accommodation space is available, local sediment supply is expected to be the controlling factor in sand ramp activity.

Individual sand ramps therefore reflect local conditions wherein sediment availability coincided with an available accommodation space. However, due to the environmental controls determining sediment dynamics, analysing multiple sand ramps in unison may provide a record of regional environmental conditions. When multiple sand ramps are analysed the local, and temporally variable, influence of accommodation space is reduced meaning periods of aeolian accumulation observed across multiple sand ramps are likely to be environmentally significant. If factors controlling sediment supply are understood, the simultaneous analysis of multiple sand ramps with geomorphically similar sediment sources may provide relatively long and stable records of Quaternary sediment dynamics, palaeoenvironmental conditions and potentially palaeoclimatic conditions in regions typically devoid of detailed Quaternary records.

Conclusions

Sand ramps are abundant along the eastern margin of the Namib Sand Sea and are present, although less common, in other locations in south west Namibia with 75 sand ramps identified in the study region (Figure 2). These sand ramps range from 150 to 3000 m in length with varying morphology and sedimentology. OSL dating indicates episodic sand ramp activity between 0.2 and >200 ka (Figure 6) although more recent ages may represent surface reworking. This confirms preliminary dates from Bertram (2003) and indicates that sand ramps are not solely Last Glacial features but existed in the Namibian landscape during the Last Interglacial, and likely before.

Analysing where sand ramps do and do not form across the varying geology and climatic gradients of the study area allowed the conditions needed for sand ramp formation to be assessed. These controls are proposed to be:

1. an adequate supply of sediment with significant aeolian transport potential;
2. an appropriate accommodation space;
3. directionally-persistent winds with sufficient energy for aeolian sand transport;
4. an arid to semi-arid climate but with sufficient seasonal, or longer term, variability to promote differing geomorphic and depositional processes

Four classes of sand ramp morphology were identified. These closely link size to complexity and indicate that the available accommodation space, and the ultimate size a sand ramp can grow to, play a large role in the morphology of the sand ramp and potentially its sensitivity to environmental change. Sediments of large sand ramps are able to stabilise as aeolian activity is refocused on secondary dune features which are able to form on the planar surface of the sand ramp. Dunes are unable to form on smaller sand ramps, leaving the surface vulnerable to reworking unless it is protected by talus.

The stratigraphy of individual sand ramps reflects local conditions wherein sediment availability coincided with available accommodation space or non-stabilised sediments were reworked. Accommodation space availability offers a purely local control on sand ramp formation whereas sediment supply provides a regional environmental picture with

ephemeral rivers representing the likely sediment source for most of the sand ramps studied.

Therefore, the primary record of individual sand ramps is local and is influenced by non-climatic controlling factors including: the size of the sand ramp, the availability of the accommodation space and the sediment supply. However, when multiple sand ramps are analysed in unison with sedimentological and morphological context, regionally common periods of accumulation can be identified. From this regional patterns of sediment dynamics, which are likely to reflect past regional climatic changes, can emerge.

Acknowledgements—Fieldwork for this project was conducted under research/collecting permit number 1787/2013 issued by the Ministry of Environment and Tourism, Namibia for which the authors are very grateful. Piet Swiegers, Brita Flinner, Swen Bachran and Richard Fryer, Petri and Hermien Oberholtzer and Vanessa and Quintin Hartung are thanked for their hospitality and local knowledge. Szilvi Bajkan is very gratefully thanked for her assistance in the lab and Sallie Burrough, Julie Durcan and the members of the OLD lab are thanked for all the interesting discussions and advice. ICP-MS and -AES measurements were made at SUREC. This work is funded by NERC PhD studentship NE/K500811/1.

References

- Aitken MJ. 1985. *Thermoluminescence Dating*. Academic Press: London.
- Al-Masrahy MA, Mountney NP. 2013. Remote sensing of spatial variability in aeolian dune and interdune morphology in the Rub' Al-Khali, Saudi Arabia. *Aeolian Research* **11**: 155–170. <https://doi.org/10.1016/j.aeolia.2013.06.004>.
- Armitage SJ, Bailey RM. 2005. The measured dependence of laboratory beta dose rates on sample grain size. *Radiation Measurements* **39**: 123–127. <https://doi.org/10.1016/j.radmeas.2004.06.008>.
- Atlas of Namibia Project. 2002. Directorate of Environmental Affairs, Ministry of Environment and Tourism (http://209.88.21.36/Atlas/Atlas_web.htm). Available from: http://www.uni-koeln.de/sfb389/e/e1/download/atlas_namibia/main_namibia_atlas.html. Accessed: 8/10/15.
- Bateman MD, Bryant RG, Foster IDL, Livingstone I, Parsons AJ. 2012. On the formation of sand ramps: a case study from the Mojave Desert. *Geomorphology* **161–162**: 93–109. <https://doi.org/10.1016/j.geomorph.2012.04.004>.
- Becker T, Schreiber U, Kampunzu AB, Armstrong R. 2006. Mesoproterozoic rocks of Namibia and their plate tectonic setting. *Journal of African Earth Sciences* **46**: 112–140. <https://doi.org/10.1016/j.jafrearsci.2006.01.015>.
- Bell WT. 1979. Attenuation factors for the absorbed radiation dose in quartz inclusions for thermoluminescence dating. *Ancient TL* **8**: 1–12.
- Berking J, Schütt B. 2011. Geoarchaeology and chronostratigraphy in the vicinity of meroitic naga in northern Sudan - a review. *eTopoi Journal for Ancient Studies* **1**: 23–43.
- Bertram S. 2003. Late quaternary sand ramps in south-western Namibia: nature, origin and palaeoclimatological significance, Unpublished PhD thesis: Universität Würzburg. Available online at: http://www.opus-bayern.de/uni-wuerzburg/606_volltexte/2003/617/pdf/Dissertation_Silke_Bertram.pdf.
- Blott SJ, Pye K. 2001. GRADISTAT: a grain size distribution and statistics package for the analysis of unconsolidated sediments. *Earth Surface Processes and Landforms* **26**: 1237–1248. <https://doi.org/10.1002/esp.261>.
- Bøtter-Jensen L, Agersnap Larsen N, Mejdahl V, Poolton NRJ, Morris MF, McKeever SWS. 1995. Luminescence sensitivity changes in quartz as a result of annealing. *Radiation Measurements* **24**: 535–541. [https://doi.org/10.1016/1350-4487\(95\)00006-Z](https://doi.org/10.1016/1350-4487(95)00006-Z).
- Bøtter-Jensen L, Andersen CE, Duller GAT, Murray AS. 2003. Developments in radiation, stimulation and observation facilities in luminescence measurements. *Radiation Measurements* **37**: 535–541. [https://doi.org/10.1016/S1350-4487\(03\)00020-9](https://doi.org/10.1016/S1350-4487(03)00020-9).
- Breed CS, Grow T. 1979. Morphology and distribution of dunes in sand seas observed by remote sensing. In *A Study of Global Sand Sea*, McKee ED (ed); 253–303. United States Geological Survey Professional Paper, 1052.
- Bristow CS, Lancaster N, Duller GAT. 2005. Combining ground penetrating radar surveys and optical dating to determine dune migration in Namibia. *Journal of the Geological Society* **162**: 315–321. <https://doi.org/10.1144/0016-764903-120>.
- Bristow CS, Duller GAT, Lancaster N. 2007. Age and dynamics of linear dunes in the Namib Desert. *Geology* **35**: 555–558. <https://doi.org/10.1130/G23369A.1>.
- Chase B. 2009. Evaluating the use of dune sediments as a proxy for palaeo-aridity: a southern African case study. *Earth-Science Reviews* **93**: 31–45. <https://doi.org/10.1016/j.earscirev.2008.12.004>.
- Chase BM, Meadows ME. 2007. Late Quaternary dynamics of southern Africa's winter rainfall zone. *Earth-Science Reviews* **84**: 103–138. <https://doi.org/10.1016/j.earscirev.2007.06.002>.
- Chase BM, Meadows ME, Scott L, Thomas DSG, Marais E, Sealy J, Reimer PJ. 2009. A record of rapid Holocene climate change preserved in hyrax middens from southwestern Africa. *Geology* **37**: 703–706.
- Chase BM, Meadows ME, Carr AS, Reimer PJ. 2010. Evidence for progressive Holocene aridification in southern Africa recorded in Namibian hyrax middens: implications for African Monsoon dynamics and the 'African humid period'. *Quaternary Research* **74**: 36–45.
- Chojnacki M, Moersch JE, Burr DM. 2010. Climbing and falling dunes in Valles Marineris, Mars. *Geophysical Research Letters* **37**: n/a–n/a. <https://doi.org/10.1029/2009GL042263>.
- Clemmensen LB, Fornós JJ, Rodríguez-perea A. 1997. Morphology and architecture of a late Pleistocene cliff-front dune, Mallorca, Western Mediterranean. *Terra Nova* **9**: 251–254. <https://doi.org/10.1111/j.1365-3121.1997.tb00023.x>.
- del Valle L, Gómez-Pujol L, Fornós JJ, Timar-gabor A, Anechitei-Deacu V, Pomar F. 2016. Middle to late Pleistocene dunefields in rocky coast settings at Cala Xuclar (Eivissa, Western Mediterranean): recognition, architecture and luminescence chronology. *Quaternary International* **407**: 4–13. <https://doi.org/10.1016/j.quaint.2016.01.050>.
- Dong Z, Qian G, Luo W, Zhang Z, Xiao S, Zhao A. 2009. Geomorphological hierarchies for complex mega-dunes and their implications for mega-dune evolution in the Badain Jaran Desert. *Geomorphology* **106**: 180–185. <https://doi.org/10.1016/j.geomorph.2008.10.015>.
- Dong Z, Wang T, Wang X. 2004. Geomorphology of the megadunes in the Badain Jaran Desert. *Geomorphology* **60**: 191–203. <https://doi.org/10.1016/j.geomorph.2003.07.023>.
- Duller GAT. 2003. Distinguishing quartz and feldspar in single grain luminescence measurements. *Radiation Measurements* **37**: 161–165. [https://doi.org/10.1016/S1350-4487\(02\)00170-1](https://doi.org/10.1016/S1350-4487(02)00170-1).
- Duller GAT. 2008. Single-grain optical dating of Quaternary sediments: why aliquot size matters in luminescence dating. *Boreas* **37**: 589–612. <https://doi.org/10.1111/j.1502-3885.2008.00051.x>.
- Durcan JA, Duller GAT. 2011. The fast ratio: a rapid measure for testing the dominance of the fast component in the initial OSL signal from quartz. *Radiation Measurements* **46**: 1065–1072. <https://doi.org/10.1016/j.radmeas.2011.07.016>.
- Durcan JA, King GE, Duller GAT. 2015. DRAC: Dose rate and age calculator for trapped charge dating. *Quaternary Geochronology* **28**: 54–61. <https://doi.org/10.1016/j.quageo.2015.03.012>.
- Ellwein AL, Mahan SA, McFadden LD. 2015. Impacts of climate change on the formation and stability of late Quaternary sand sheets and falling dunes, Black Mesa region, southern Colorado Plateau, USA. *Quaternary International* **362**: 87–107. <https://doi.org/10.1016/j.quaint.2014.10.015>.
- Ewing RC, Kocurek G, Lake LW. 2006. Pattern analysis of dune-field parameters. *Earth Surface Processes and Landforms* **31**: 1176–1191. <https://doi.org/10.1002/esp.1312>.
- Fitzsimmons KE, Rhodes EJ, Barrows TT. 2010. OSL dating of southeast Australian quartz: a preliminary assessment of luminescence characteristics and behaviour. *Quaternary Geochronology* **5**: 91–95. <https://doi.org/10.1016/j.quageo.2009.02.009>.
- Folk RL, Ward WC. 1957. Brazos river bar: a study in the significance of grain size parameters. *Journal of Sedimentary Petrology* **27**: 3–26.
- Galbraith RF. 1999. Optical dating of single and multiple grains of quartz from jinnium rock shelter, northern australia: part i, experimental design and statistical models. *Archaeometry* **2**: 339–364.

- Galehouse JS. 1971. Point counting. In *Procedures in Sedimentary Petrology*, Carver RE (ed). Wiley: New York; 385–407.
- Garzanti E, Andò S. 2007. Heavy-mineral concentration in modern sands: implications for provenance interpretation. In *Mesoproterozoic Rocks of Namibia and their Plate Tectonic Setting*, Mange MA, Wright DT (eds). Elsevier: Amsterdam; 517–545.
- Garzanti E, Andò S, Vezzoli G, Lustrino M, Boni M, Vermeesch P. 2012. Petrology of the Namib Sand Sea: long-distance transport and compositional variability in the wind-displaced Orange Delta. *Earth-Science Reviews* **112**: 173–189. <https://doi.org/10.1016/j.earscirev.2012.02.008>.
- Geyh MA, Heine K. 2014. Several distinct wet periods since 420ka in the Namib Desert inferred from U-series dates of speleothems. *Quaternary Research* **81**: 381–391. <https://doi.org/10.1016/j.yqres.2013.10.020>.
- Goudie AS. 2013. *Arid and Semi-Arid Geomorphology*. Cambridge University Press: Cambridge.
- Guérin G, Mercier N, Nathan R, Adamiec G, Lefrais Y. 2012. On the use of the infinite matrix assumption and associated concepts: a critical review. *Radiation Measurements* **47**: 778–785. <https://doi.org/10.1016/j.radmeas.2012.04.004>, <https://doi.org/10.1016/j.radmeas.2012.04.004>.
- Heiri O, Lotter AF, Lemcke G. 2001. Loss on ignition as a method for estimating organic and carbonate content in sediments: reproducibility and comparability of results. *Journal of Paleolimnology* **25**: 101–110. <https://doi.org/10.1023/A:1008119611481>.
- Kumar A, Srivastava P, Meena NK. 2016. Late Pleistocene aeolian activity in the cold desert of Ladakh: a record from sand ramps. *Quaternary International*. <https://doi.org/10.1016/j.quaint.2016.04.006>.
- Lancaster J, Lancaster N, Seely MK. 1984. Climate of the central Namib desert. *Madoqua* **14**: 5–61.
- Lancaster N. 1985. Winds and sand movements in the Namib Sand Sea. *Earth Surface Processes and Landforms* **10**: 607–619.
- Lancaster N. 1988. The development of large aeolian bedforms. *Sedimentary Geology* **55**: 69–89. [https://doi.org/10.1016/0037-0738\(88\)90090-5](https://doi.org/10.1016/0037-0738(88)90090-5).
- Lancaster N. 2002. How dry was dry? Late Pleistocene palaeoclimates in the Namib Desert. *Quaternary Science Reviews* **21**: 769–782.
- Lancaster N. 2009. Dune morphology and dynamics. In *Geomorphology of Desert Environments*, Parsons AJ, Abrahams AD (eds). Springer: Amsterdam; 557–595.
- Lancaster N, Tchakerian VP. 1996. Geomorphology and sediments of sand ramps in the Mojave desert. *Geomorphology* **17**: 151–165. [https://doi.org/10.1016/0169-555X\(95\)00101-A](https://doi.org/10.1016/0169-555X(95)00101-A).
- Lim S, Chase BM, Chevalier M, Reimer PJ. 2016. 50 000 years of vegetation and climate change in the southern Namib Desert, Pella, South Africa. *Palaeogeography, Palaeoclimatology, Palaeoecology* **451**: 197–209.
- Liritzis I, Stamoulis K, Papachristodoulou C, Ioannidea K. 2013. A re-evaluation of radiation dose-rate conversion factors. *Mediterranean Archaeology and Archaeometry* **13**: 1–15.
- Livingstone I, Bristow C, Bryant RG, Bullard J, White K, Wiggs GFS, Baas ACW, Bateman MD, Thomas DSG. 2010. The Namib Sand Sea digital database of aeolian dunes and key forcing variables. *Aeolian Research* **2**: 93–104. <https://doi.org/10.1016/j.aeolia.2010.08.001>.
- Morton AC, Hallsworth CR. 1999. Processes controlling the composition of heavy mineral assemblages in sandstones. *Sedimentary Geology* **124**: 3–29. [https://doi.org/10.1016/S0037-0738\(98\)00118-3](https://doi.org/10.1016/S0037-0738(98)00118-3).
- Moska P, Murray AS. 2006. Stability of the quartz fast-component in insensitive samples. *Radiation Measurements* **41**: 878–885. <https://doi.org/10.1016/j.radmeas.2006.06.005>.
- Netterberg AF. 1969. The Interpretation of some basic calcrete types. *The South African Archaeological Bulletin* **24**: 117–122.
- Nicholson SE. 2000. The nature of rainfall variability over Africa on time scales of decades to millenia. *Global and Planetary Change* **26**: 137–158. [https://doi.org/10.1016/S1350-4487\(00\)00055-X](https://doi.org/10.1016/S1350-4487(00)00055-X).
- Pease PP, Tchakerian VP. 2003. Geochemistry of sediments from Quaternary sand ramps in the southeastern Mojave Desert, California. *Quaternary International* **104**: 19–29. [https://doi.org/10.1016/S1040-6182\(02\)00132-5](https://doi.org/10.1016/S1040-6182(02)00132-5).
- Pietsch TJ, Olley JM, Nanson GC. 2008. Fluvial transport as a natural luminescence sensitiser of quartz. *Quaternary Geochronology* **3**: 365–376. <https://doi.org/10.1016/j.quageo.2007.12.005>.
- Poolton NRJ, Smith GM, Riedi PC, Bulur E, Bøtter-Jensen L, Murray AS, Adrian M. 2000. Luminescence sensitivity changes in natural quartz induced by high temperature annealing: a high frequency EPR and OSL study. *Journal of Physics D: Applied Physics* **33**: 1007–1017. <https://doi.org/10.1088/0022-3727/33/8/318>.
- Prescott JR, Hutton JT. 1994. Cosmic ray contributions to dose rates for luminescence and ESR dating: large depths and long-term time variations. *Radiation Measurements* **23**: 497–500. [https://doi.org/10.1016/1350-4487\(94\)90086-8](https://doi.org/10.1016/1350-4487(94)90086-8).
- Pye K, Tsoar H. 1990. *Aeolian Sand and Sand Dunes*. Unwin Hyman: London.
- Qian G, Dong Z, Luo W, Lu J. 2011a. Mean airflow patterns upwind of topographic obstacles and their implications for the formation of echo dunes: a wind tunnel simulation of the effects of windward slope. *Journal of Geophysical Research* **116**: F04026. <https://doi.org/10.1029/2011JF002020>.
- Qian G, Dong Z, Luo W, Zhang Z, Zhao A. 2011b. Airflow patterns upwind of obstacles and their significance for echo dune formation: a field measurement of the effects of the windward slope angle. *Science China-Earth Sciences* **55**: 545–553. <https://doi.org/10.1007/s11430-011-4248-4>.
- Rendell HM, Sheffer NL. 1996. Luminescence dating of sand ramps in the Eastern Mojave Desert. *Geomorphology* **17**: 187–197. [https://doi.org/10.1016/0169-555X\(95\)00102-B](https://doi.org/10.1016/0169-555X(95)00102-B).
- Sawakuchi AO, Blair MW, DeWitt R, Faleiros FM, Hyppolito T, Guedes CCF. 2011a. Thermal history versus sedimentary history: OSL sensitivity of quartz grains extracted from rocks and sediments. *Quaternary Geochronology* **6**: 261–272. <https://doi.org/10.1016/j.quageo.2010.11.002>.
- Sawakuchi AO, DeWitt R, Faleiros FM. 2011b. Correlation between thermoluminescence sensitivity and crystallization temperatures of quartz: potential application in geothermometry. *Radiation Measurements* **46**: 51–58. <https://doi.org/10.1016/j.radmeas.2010.08.005>.
- Stone AEC. 2013. Age and dynamics of the Namib Sand Sea: a review of chronological evidence and possible landscape development models. *Journal of African Earth Sciences* **82**: 70–87. <https://doi.org/10.1016/j.jafrearsci.2013.02.003>.
- Stone AEC, Thomas DSG. 2008. Linear dune accumulation chronologies from the southwest Kalahari, Namibia: challenges of reconstructing late Quaternary palaeoenvironments from aeolian landforms. *Quaternary Science Reviews* **27**: 1667–1681. <https://doi.org/10.1016/j.quascirev.2008.06.008>.
- Stone AEC, Thomas DSG, Viles HA. 2010a. Late Quaternary palaeohydrological changes in the northern Namib Sand Sea: new chronologies using OSL dating of interdigitated aeolian and water-lain interdune deposits. *Palaeogeography, Palaeoclimatology, Palaeoecology* **288**: 35–53. <https://doi.org/10.1016/j.palaeo.2010.01.032>.
- Stone AEC, Viles HA, Thomas L, Van Calsteren P. 2010b. Can 234U–230Th dating be used to date large semi-arid tufas? Challenges from a study in the Naukluft Mountains, Namibia. *Journal of Quaternary Science* **25**: 1360–1372. <https://doi.org/10.1002/jqs.1435>.
- Telfer MW, Mills SC, Mather AE. 2014. Extensive Quaternary aeolian deposits in the Drakensberg foothills, Rooiberge, South Africa. *Geomorphology* **219**: 161–175. <https://doi.org/10.1016/j.geomorph.2014.05.006>.
- Telfer MW, Thomas DSG. 2007. Late Quaternary linear dune accumulation and chronostratigraphy of the southwestern Kalahari: implications for aeolian palaeoclimatic reconstructions and predictions of future dynamics. *Quaternary Science Reviews* **26**: 2617–2630. <https://doi.org/10.1016/j.quascirev.2007.07.006>.
- Telfer MW, Thomas ZA, Breman E. 2012. Sand ramps in the Golden Gate Highlands National Park, South Africa: evidence of periglacial aeolian activity during the last glacial. *Palaeogeography, Palaeoclimatology, Palaeoecology* **313–314**: 59–69. <https://doi.org/10.1016/j.palaeo.2011.10.008>.
- Thomas DSG, Bateman MD, Mehrshahi D, O'hara SL. 1997. Development and environmental significance of an eolian sand

- ramp of last-glacial age, Central Iran. *Quaternary Research* **48**: 155–161. <https://doi.org/10.1006/qres.1997.1923>.
- Thomas DSG, Burrough SL. 2012. Interpreting geoproxies of late Quaternary climate change in African drylands: implications for understanding environmental and early human behaviour. *Quaternary International* **253**: 5–17. <https://doi.org/10.1016/j.quaint.2010.11.001>.
- Tsoar H. 1983. Wind tunnel modelling of echo and climbing dunes. In *Eolian Sediments and Processes*, Brookfield ME, Ahlbrandt TS (eds). Elsevier: Amsterdam; 247–259.
- Turner BR, Makhoulf I. 2002. Recent colluvial sedimentation in Jordan: fans evolving into sand ramps. *Sedimentology* **49**: 1283–1298. <https://doi.org/10.1046/j.1365-3091.2002.00497.x>.
- Tyson PD, Seely MK. 1980. Local winds over the central Namib Desert. *South African Geographical Journal* **62**: 136–150.
- Warren A, Allison D. 1998. The palaeoenvironmental significance of dune size hierarchies. *Palaeogeography, Palaeoclimatology, Palaeoecology* **137**: 289–303. [https://doi.org/10.1016/S0031-0182\(97\)00110-7](https://doi.org/10.1016/S0031-0182(97)00110-7).
- Wintle AG, Murray AS. 2006. A review of quartz optically stimulated luminescence characteristics and their relevance in single-aliquot regeneration dating protocols. *Radiation Measurements* **41**: 369–391. <https://doi.org/10.1016/j.radmeas.2005.11.001>.
- Wold S, Esbensen K, Geladi P. 1987. Principal component analysis. *Chemometrics and Intelligent Laboratory Systems* **2**: 37–52. [https://doi.org/10.1016/0169-7439\(87\)80084-9](https://doi.org/10.1016/0169-7439(87)80084-9).
- Wright VP. 2007. Calcrete. In *Geochemical Sediments and Landscapes*, Nash DJ, McLaren SJ (eds). Blackwell: Oxford; 10–45.
- Xianwan L, Sen L, Jianyou S. 1999. Wind tunnel simulation experiment of mountain dunes. *Journal of Arid Environments* **42**: 49–59. <https://doi.org/10.1006/jare.1998.0488>.

Supporting Information

Additional Supporting Information may be found online in the supporting information tab for this article.